Solar Wind Radiation Damage Effects in Lunar Material

Final Technical Report

N72-14807 (NASA-CR-115309) SOLAR WIND RADIATION DAMAGE EFFECTS IN LUNAR MATERIAL Lunar Sample Analysis Program. Final Technical Report B. Hapke, et al (Pittsburgh Univ.) 30 Nov. 1971 71 p CSCL 03B G3/29

Unclas
11215

FACIL (NASA CR OR TMX OR AD NUMBER) (CATEGORY)

OFFICE OF PRIME RESPONSIBILITY

TA

OPEN

NATIONAL AERONAUTICS AND SPACE ADMINISTRATION

LUNAR SAMPLE ANALYSIS PROGRAM

Solar Wind Radiation Damage Effects in Lunar Material

Final Technical Report

November 30, 1971

Principal Investigator: Bruce Hapke

Co-Investigators: Alvin J. Cohen and William A. Cassidy

Contract NAS 9-9942

Department of Earth and Planetary Sciences
University of Pittsburgh
Pittsburgh, Pennsylvania 15213

Prepared for

NATIONAL AERONAUTICS AND SPACE ADMINISTRATION
Manned Space Craft Center
Lunar Receiving Laboratory
Houston, Texas

This report, together with the enclosed reprints and preprints, summarizes and describes the research accomplished under NASA Contract NAS 9-9942 on solar wind radiation damage and other effects in lunar samples. The primary purpose of this research project was to try to improve our understanding of the optical properties of lunar materials and in particular to learn how these properties may have been effected by radiation.

The results of this research have been reported in the following papers, a copy of each of which is enclosed:

"Solar Radiation Effects in Lunar Samples", B. Hapke, A. Cohen, W. Cassidy and E. Wells, Science, 167, 745 (1970).

"Solar Radiation Effects on the Optical Properties of Apollo 11 Samples", B. Hapke, A. Cohen, W. Cassidy and E. Wells, Proceedings of the Apollo 11 Lunar Science Conference, 2199 (1970).

"The Albedo of the Moon: Evidence for Vapor Phase Deposition Processes on the Lunar Surface", B. Hapke, W. Cassidy and E. Wells, presented at the Second Lunar Science Conference, Houston, Texas, January, 1971.

"Radiation Effects in Lunar Crystaline Rocks", A. J. Cohen, presneted at the Second Apollo Lunar Science Conference, Houston, Texas, January, 1971.

"The Valence States of 3d Transition Elements in Apollo 11 and 12 Rocks", A. J. Cohen, presented at IAU Symposium 47 on The Moon, University of New Castle, March, 1971.

"Progress in Understanding the Optical Spectra of Lunar Materials", B. Hapke, W. Cassidy and E. Wells, presented at the Conference on Lunar Geophysics, Houston, Texas, October, 1971.

"Trace Ferric Iron in Lunar and Meteoritic Titanaugites", A. J. Cohen, presented at Conference on Lunar Geophysics, Houston, Texas, October, 1971.

Reprinted from
30 January 1970, Volume 167, pp. 745-747

SCIENCE

Apollo 11 Lunar Science Conference

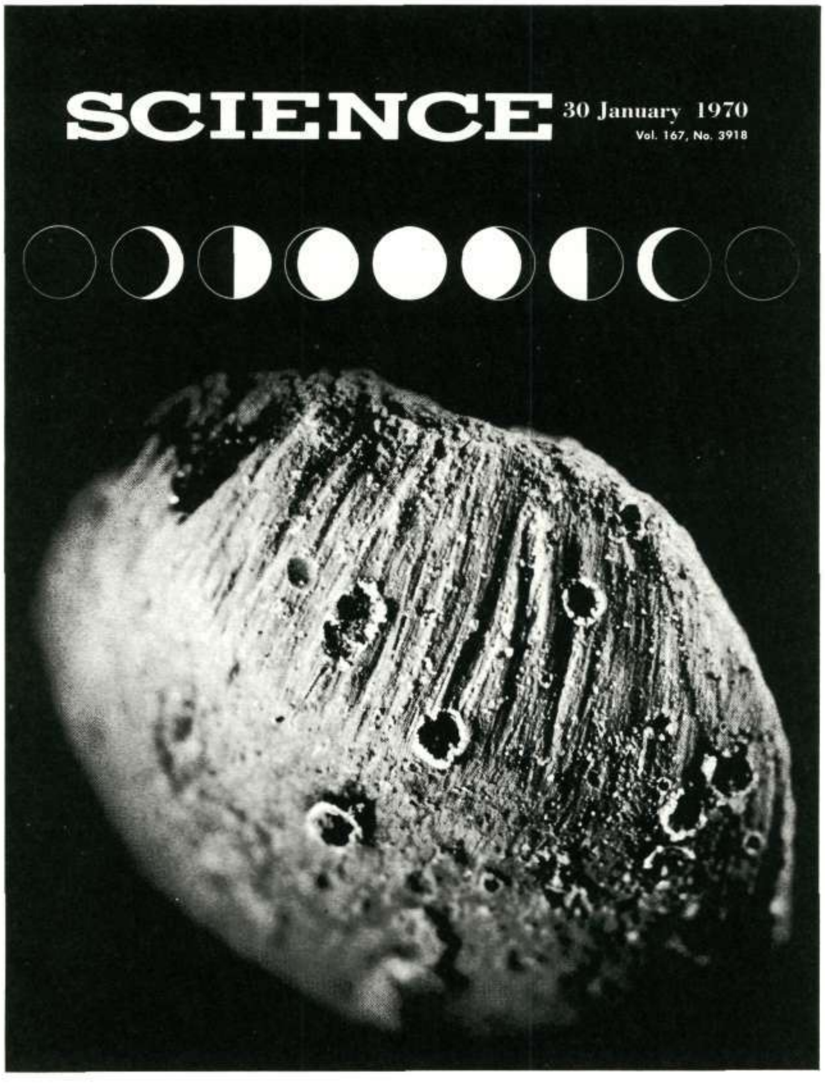

Solar Radiation Effects in Lunar Samples

B. W. Hapke, A. J. Cohen, W. A. Cassidy and E. N. Wells

Solar Radiation Effects in Lunar Samples

Abstract. *Optical properties of the pulverized crystalline rocks from the Apollo 11 samples are different from the optical properties of lunar soil. Changes in these properties were induced in the samples by ultraviolet and x-irradiation, standing, and heating. The albedo and spectrum of the soil differed significantly from expected values.*

The purpose of our work is to ascertain the possible role that various types of radiation may have played in determining the optical properties of the lunar surface. We investigated the effects of low-energy protons, ultraviolet and x-ray irradiation, heating, particle size, composition, and packing on the albedos and spectra of the samples.

The particle size distribution in fines sample 10084,81 was measured by sieving and sedimentation. The median particle size, weighted by mass, was about 40 μm, with over 35 percent of the mass contained in particles smaller than 20 μm. These results are in agreement with a previous size determination (*1*) and with estimates of "mean particle size of a few tens of microns or less" (*2*), based on telescopic optical data.

According to Wildey (*3*) the 0° phase angle albedo of the moon in the vicinity of the Apollo 11 site is approximately 0.099. Correcting this value for photometric function to a 6° phase angle gives 0.079. However, the subsurface soil appears to be darker than the surface material by 5 to 30 percent, depending on location (*4*). Since most of the sample presumably came from below the surface, a 6° albedo in the range of 0.060 to 0.076 is thus to be expected. The actual measured value relative to MgO is 0.090. The degree of compaction of the material cannot reduce this value sufficiently. We conclude that the returned sample of fines may not be representative of the general region of the moon around Tranquillity Base, at least as far as the factors that determine albedo are concerned.

The reflection spectrum of the fines, as measured by a Cary 14 spectrophotometer, is shown in Fig. 1 along with the general spectrum of the moon (*5*). The general lunar spectrum is considerably redder than the spectrum of the fines. We are not certain of the reason for this discrepancy; it may reflect errors in our measuring techniques, or it may indicate that this material is not typical of the surface of the moon as a whole, possibly because of alteration processes acting on the lunar surface or changes which occurred during or after collection. There is no sign in the fines of the 290-nm band reported in the lunar spectrum. We caution that the apparent peak at 250 nm in our data may be spurious. However, an absorption band at 900 to 1000 nm due to Fe^{2+} is clearly present in the spectrum of the fines.

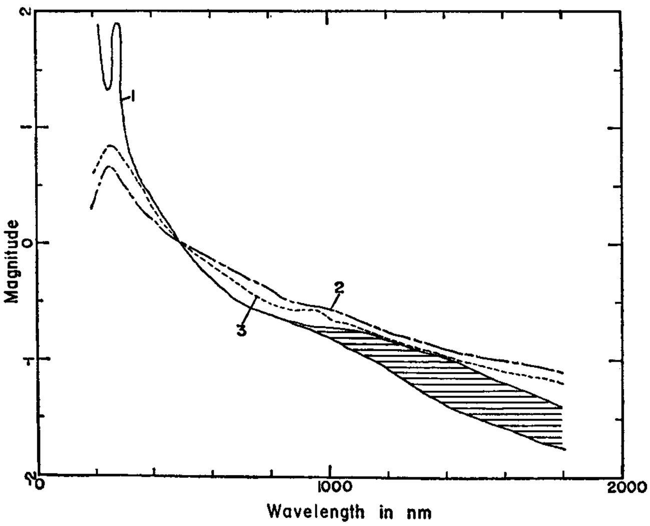

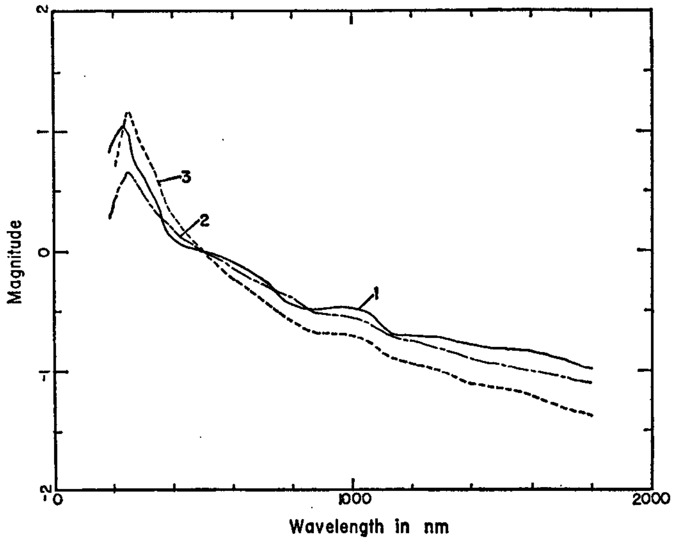

Fig. 1 (left). Relative reflection spectra, in magnitudes, of lunar materials, normalized at 500 nm; curve 1, average moon; curve 2, fines; curve 3, fines after ultraviolet irradiation. Fig. 2 (right). Relative reflection spectra, in magnitudes, of lunar materials, normalized at 500 nm; curve 1, pulverized crystalline rock 10022; curve 2, fines; curve 3, powdered rock after H-ion irradiation.

The lunar soil is commonly thought to be derived from larger fragments of lunar surface material by meteorite comminution. We attempted to ascertain whether the parent rocks of the soil could be identified by reflection spectra. Chips of all rocks received in our original allocation (numbers 10017 and 10022, crystalline, and 10048 and 10065, breccia) were ground to finer than 37 μm. The spectra and albedos of the powdered breccias are similar to those of the fines; however, these rocks are probably daughter products of the soil, formed by impact, rather than the parent rocks.

The crystalline rock powders are twice as bright as the fines, with albedos of 0.183; also the spectra of the two materials show significant differences (Fig. 2). However, the rocks and the fines are chemically quite similar (*1*). We emphasize that four rocks constitute too small a sample on which to base firm conclusions. However, if the crystalline rocks are indeed representative of the parents of the fines, then the optical properties of the crystalline rock powder must have been altered by some factor in the lunar environment.

It is suggestive that the albedo of the crystalline rock flour is similar to the albedo of the brighter rays on the moon. We also point out that several of the small differences between the spectra of various regions on the moon (*6*) can be accounted for if varying amounts of unaltered crystalline rocks or flour are exposed on the lunar surface.

It has been suggested that the solar wind is responsible for the low albedo and reddish color of the lunar soil (*7*). Therefore, a pulverized sample of crystalline rock 10022 was irradiated by approximately 20 coulomb/cm^2 of 2-kev hydrogen ions. This treatment reduced the albedo of the flour from 0.18 to 0.12, and the spectrum became more red, as shown in Fig. 2. This irradiation was conducted in a vacuum system constructed only of metal and ceramic components and evacuated by a sputter-ion pump with molecular-sieve roughing.

A sample of fines was subjected to intense ultraviolet and visible radiation from a 200-watt Oriel xenon-mercury lamp for 16 hours. This treatment (the dose has not yet been calibrated) increased the albedo from 0.090 to 0.096 and altered the spectrum of the soil (Fig. 1). Probably Fe^{2+} ions in the material were oxidized to Fe^{3+} by radiation, with a resulting decrease of absorption in the visible and near-infrared and increase in the ultraviolet.

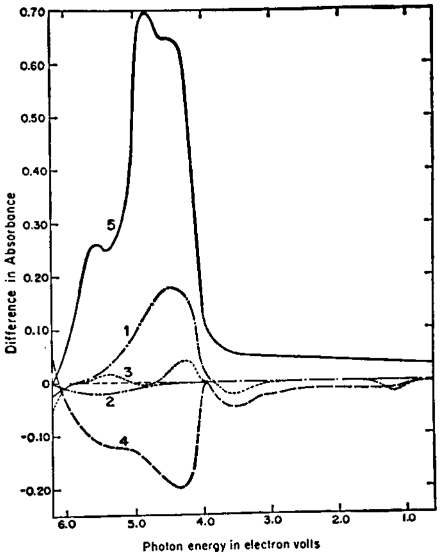

Fig. 3. Changes in absorption spectrum of lunar rock 10017 caused by radiation; curve 1, difference after ultraviolet treatment; curve 2, difference after x-irradiation from ultraviolet treatment; curve 3, difference after standing 330 hours after x-irradiation; curve 4, difference after heating at 200°C from standing; curve 5, difference after heating at 500°C from heating at 200°C.

The ultraviolet irradiation was carried out in air, and during this time the sample was heated to 160°C. To ascertain that the oxidation was not due to heating, another sample of soil was heated to 200°C in air; no change in albedo or in reflection spectrum occurred.

These radiation-induced changes were studied more quantitatively by measuring the changes in the absorption spectrum of a polished thin section of crystalline rock 10017, approximately 1 by 1 by 0.001 cm (*8*). The polished specimen of crystalline rock contained opaque ilmenite and three major transparent minerals: colorless plagioclase and two varieties of light brown pyroxenes. The spectra reported here are most probably spectra of the pyroxenes.

The spectrum of the sample before any treatment other than cutting and polishing showed the typical spectrum of ferrous ions in the near-infrared region and intense absorption due to ferric ions in the far-ultraviolet.

Because these spectra were similar to spectra of ferrous and ferric ions in synthetic quartz (*9*), we decided to use quartz as a lunar model and to perform experiments similar to earlier experiments.

Treatment of the specimen with unfiltered light of the xenon-mercury lamp for 23 hours resulted in the change shown in Fig. 3, curve 1. By subtracting the spectrum obtained before this ultraviolet treatment from the spectrum taken after treatment, we obtained the difference spectrum, which illustrates changes in the 1- to 6-ev region of the spectrum. Although no noticeable decrease had taken place in the ferrous region between 1 and 1.5 ev, there was a growth in the ferric region of the spectrum centered near 4.5 ev. The lunar rock wafer was next x-irradiated at 45-kv peak, 35 ma, with a Machlett AEG50T tube for 6 hours about 2 cm below the beryllium window. The difference induced by the x-ray treatment is shown in Fig. 3, curve 2. A decrease in the absorption spectrum took place in the ferric region centered near 5.5 ev. The specimen was allowed to stand at room temperature for 330 hours in subdued light. A decrease in the ferrous band occurred, accompanied by increase in two bands in the ferric region as shown in Fig. 3, curve 3. Heating the specimen for 2 hours at 200°C caused a large decrease in the region of the same two bands that increased previously (Fig. 3, curve 4). The specimen on standing showed decreased absorption on the deep ultraviolet and in the 3- to 4-ev region. This region decreased further on heating although the far ultraviolet showed an increase. As shown in Fig. 3, curve 5, heat treatment at 500°C in air for 2 hours caused an intense development of the α, β, and γ bands of the ferric ion (*9*). We interpret these results as follows.

If we take iron in quartz as a model, (i) ultraviolet treatment caused oxidation of ferrous ion with development of the β and γ ferric bands; (ii) x-ray treatment caused a reduction of ferric ion as shown by decrease in the α ferric band; (iii) standing caused slight oxidation of ferrous to ferric as shown by increase of α and γ ferric bands and decrease in the ferrous band; (iv) heating at 200°C caused a readjustment in the structure with possible oxidation of titanium, as indicated by increase at the ultraviolet cutoff, and decrease in the intensity of the ferric α, β, and γ bands; (v) heating at 500°C for 2 hours caused oxidation of probably most of the remaining ferrous ion with appearance of intense α, β, and γ bands of ferric ion. The trace ferric ion with high oscillator strength shows greater total change in absorbance than the abundant ferrous ion of low oscillator strength.

We conclude that these effects take

place primarily in the iron-containing pyroxenes, which are quite sensitive to radiation and temperature (in air) and should be a dynamic system when subjected to the direct solar wind even in vacuum.

Ever since the successful landing of Surveyor 1 it has been observed that gentle disturbance of the lunar soil, except by compression, results in a material which is as much as 30 percent darker than the undisturbed surface (*4*). We attempted to test several of the proposed explanations for this effect.

1) *Ultraviolet bleaching* (*10*). Ultraviolet irradiation of the soil caused albedo increases of approximately 6 percent; this value is of the same order as the disturbance effect observed by Surveyor 5.

2) *Packing.* The albedo of the soil is affected by the micromorphology of the surface in the sense that the looser the packing, the lower the albedo. The following albedos were obtained, depending on surface preparation: (i) sifted, 0.085; raked with a needle, 0.087; spooned onto a plate, 0.090; jarred by dropping the container from a height of about 5 cm, 0.094; tamped by pressing gently with the flat side of a spatula, 0.10. Since the lunar soil is continually stirred by micrometeorites it is doubtful that the natural condition of the surface is similar to that produced by tamping. Thus packing effects apparently are capable of altering the albedo by up to 10 percent.

3) *Particle size* (*11*). The albedos of fractions of fines separated as to particle size by dry sieving were measured with the following results: >149 μm, 0.089; 74 to 149 μm, 0.081; 37 to 74 μm, 0.080; < 37 μm, 0.079; unseparated, 0.090. Hence albedo differences of about 10 percent might be possible if the upper layer of particles are larger on the average than those below the surface.

4) *Lunar varnish* (*12*). Samples of the fines were examined with an optical microscope, a scanning-electron microscope, and an electron microprobe for coatings of dark material which might be scrubbed off by solar wind sputtering, but no definite evidence for such coatings was found. However, under high magnification the surfaces of many grains exhibited peculiar textures, which we were unable to interpret. These may indicate the presence of an amorphous coating on parts of some grains. In order to test the possibility that coatings of carbonaceous material might be present, a thermogravimetric analysis was carried out by heating a soil sample to 1200°C in air and measuring the change in weight (*13*). The weight of the sample increased continuously and monotonically with temperature because of oxidation, and no decrease, such as might be caused by ignition of a carbonaceous coating, was observed at any temperature.

5) *Conclusion.* Although several effects can alter the albedo of the lunar soil by up to 10 percent, none of the hypotheses yet advanced to explain the disturbance effect seem capable of completely accounting for all observations, but any or all of the hypotheses discussed here may contribute.

B. W. HAPKE, A. J. COHEN
W. A. CASSIDY, E. N. WELLS
Department of Earth and Planetary Sciences, University of Pittsburgh, Pittsburgh, Pennsylvania 15213

References and Notes

1. Lunar Sample Preliminary Examination Team, *Science* **165**, 1211 (1969).
2. B. Hapke, *Planet. Space Sci.* **16**, 101 (1968).
3. R. Wildey, private communication.
4. L. Jaffe *et al.*, *J. Geophys. Res.* **73**, 7165 (1968); E. Shoemaker *et al.*, *ibid.* **74**, 6081 (1969).
5. B Hapke, in *Physics and Astronomy of the Moon*, Z. Kopal, Ed. (Academic Press, New York, ed. 2, 1970), vol. 1, p. 72.
6. T. McCord, *J. Geophys. Res.* **74**, 3131 (1969); ———, T. Johnson, H. Kiefer, *ibid.*, p. 4358; T. McCord and T. Johnson, *ibid.*, p. 4395.
7. B. Hapke and H. Van Horn, *J. Geophys, Res.* **68**, 4545 (1963).
8. Sample preparation by G. Moreland, U.S. National Museum.
9. A. J. Cohen and F. Hassan, *Science* **167**, 176 (1970).
10. A. J. Cohen and B. Hapke, *ibid.* **161**, 1237 (1968).
11. A. Felice, *J. Geophys. Res.* **72**, 5721 (1967).
12. E. Shoemaker *et al.*, *J. Geophys. Res.* **73**, 3989 (1968).
13. We thank G. Aubele and the Fisher Scientific Company for performing this analysis.
14. We thank B. Greenspan and F. Hassan for assistance. Supported by NASA contract NAS 9-9942.

4 January 1970; revised 6 January 1970

Trace Ferric Ion in Lunar and Meteoritic Titanaugites

Alvin J. Cohen
Department of Earth and Planetary Sciences
University of Pittsburgh
Pittsburgh, Pennsylvania 15213

ABSTRACT

Evidence for presence of Fe^{3+} in lunar rocks is furnished by heating them in air to 200-225°C for two hours. This causes a large decrease in the same charge transfer bands attributed to Fe^{3+} that can be enhanced by heating the same rocks in air at 500°C. This data is interpreted as evidence that the Fe^{3+} was not in equilibrium in the melt but was produced by cosmic radiation subsequent to the rock formation. The decrease of the Fe^{3+} charge-transfer bands is accompanied by decrease in intensity of spin-allowed Fe^{2+} bands attributed to M_1 sites in the pyroxene in rock 12018. This decrease in the Fe^{2+} bands is attributed to decrease in the $Fe^{2+} \rightarrow Fe^{3+}$ charge-transfer intensification of these Fe^{2+} spin-allowed transitions when radiation-produced Fe^{3+} is partially-reduced by the low temperature heating.

The reaction of Fe^{3+} on heating to 200-225°C is probably:

$$Fe^{3+} + Ti^{3+} \rightarrow Fe^{2+} + Ti^{4+}.$$

This is the reverse of the reaction caused by cosmic ray bombardment of the rock on the lunar surface. Possible tetrahedrally coordinated Fe^{3+} is present in the meteoritic and lunar augites as suggested by comparison of their spectra to that of terrestrial augite high in Fe^{3+}. This would have been present in the original melt and is distinct from radiation produced Fe^{3+} in the M-sites.

The polarized absorption spectra of single crystal pigeonite and augite from rock 12021 before heating, and augite from 12018 after heating are compared

to that of meteoritic titanaugite in the Angra dos Reis meteorite and terrestrial titanaugite from Maui, Hawaii. The absorption spectrum of meteoritic hypersthene (Tatahouine) is also included for comparison to the pigeonite.

INTRODUCTION

It has been shown earlier (1) that heating lunar rocks at 200-225°C for 2 hours causes a large decrease in three major charge transfer bands of Fe^{3+} near 2750, 2600 and 2200A. This is accompanied by a decrease near 6800A and possibly 4675A of Ti^{3+} charge transfer bands (2). It has been concluded that this low heating causes the reaction

$$Fe^{3+} + Ti^{3+} \rightarrow Fe^{2+} + Ti^{4+} \quad (a)$$

to take place, indicating that the Fe^{3+} and Ti^{3+} are not in equilibrium. This led the writer to conclude that the Fe^{3+} and Ti^{3+} are produced by radiation, most likely cosmic rays (2) according to the following reaction:

$$Fe^{2+} (M_1, M_2) + Ti^{4+} (z, M_1) \rightarrow Fe^{3+} (M_1, M_2) + Ti^{3+} (z, M_1) \quad (b).$$

The Fe^{3+} produced would be at the M_1 and M_2 sites of Fe^{2+}, one Ti^{4+} being reduced for each Fe^{2+} oxidized. The Ti^{4+} could be at either M_1 or the z (Si^{4+} tetrahedral) site. It was noted that on heating, as the Ti^{3+} decreased, the absorption in the region near the ultraviolet cut-off increased; this is attributed to increase in Ti^{4+} during oxidation of Ti^{3+} upon mild heating (1).

It was found that as Fe^{3+} charge transfer bands decreased in lunar rocks 10017, 10022 and 12018 upon heating to 200-225°C for 2 hours, bands in the Fe^{2+} region of the spectrum also decreased as shown in Table 1. This was unexpected as one would expect that bands in this region would increase slightly or remain unchanged as the Fe^{3+} was reduced depending on the comparative oscillator strengths of the Fe^{3+} charge transfer bands and Fe^{2+} spin allowed d-transitions. That the Fe^{2+} region showed a decrease could only be interpreted that there was an interaction between the Fe^{3+} charge transfer levels and the spin allowed d levels of Fe^{2+}.

In this paper the charge transfer spectral transitions of Fe^{3+}, will be given tentative structural locations based on changes during heating and other radiation effects (3). No evidence as to the nature of charge transfer has been detected, although these bands are similar to ones for Fe^{3+} in quartz (4). In Table 1 the probable site positions in the augite structure are given for the Fe^{3+} charge transfer bands based on the effect of mild heating.

There are three different possible sites for Fe^{3+} in the diopside structure of augite, M_1, the major site of Mg^{2+}, M_2, the major site of Ca^{2+}, and z, the tetrahedral Si^{4+} site. The M_1 site is the octahedral site preferred by Fe^{3+} in the diopside structure (5). Fe^{3+} will also follow Al^{3+} into the z site. The Fe^{2+} ion prefers the M_2 site, will occupy the M_1 site, and cannot occupy the z site due to its size and the charge difference of +2 from Si^{4+} (6).

Since Fe^{2+} cannot occupy the tetrahedral site (this does not pertain to possible Fe^{2+} produced from Fe^{3+} by radiation-reduction but to entry into the z site as the crystal is formed from the melt) but Fe^{3+} can, heating of minerals should not affect the Fe^{3+} in this site. However Fe^{3+} produced by radiation damage by oxidation of Fe^{2+} in M_1 and M_2-sites should be reduced on heating with oxidation of an equal quantity of Ti^{3+}. Since bands at 2700-2850A show a large decrease upon heating to 200-225°C as do bands at 2200-2250A, these are likely due to Fe^{3+} at M_1 or M_2 sites. The bands at 2600-2700A are unresolved upon heating at 200-225°C and probably undergo no change. Charge transfer bands in this region are therefore assigned to Fe^{3+} in a tetrahedral site. Since the energy diagram of the charge transfer spectrum of Fe^{3+} has not been explored it is not known if the other two bands are two transitions at one 6-coordinate site or one each from the M_1 and M_2 site, respectively. Tentatively the 2700-2850A band will be assigned to an M_1 site and the 2200-2250 band to an M_2 site, until further radiation experiments can elucidate this problem. Preliminary data (1,3) indicates that the 2200-2250A band is reduced by X-ray treatment which is more likely for Fe^{3+} in an M_2 site preferred by Fe^{2+}. The same set of experiments indicates that treatment with UV light causes an increase mainly in the 2700-2850A band. It is expected that the oxidation of Fe^{2+} in an M_1 site would have lower

Table 1

Effect of Heating at 200-225°C on Charge Transfer Bands of Fe^{3+} in Lunar Rocks

C. T. Band	Rock No.	Mineral	Possible Mineral Site	Absorbance Change
2750A	10017,52	Augite	M_1	large decrease
	10022,48	Augite	M_1	large decrease band unresolved
2850	12018,50	Augite	M_1	data unavailable
2700	12021,65	Augite	M_1	data unavailable
2750	12021,65	Pigeonite	M_1	data unavailable
2250	10017,52	Augite	M_2	large decrease
2250	10022,48	Pigeonite Augite	M_2	large decrease
2200	12018,50	Augite	M_2	unresolved, prob. large decrease
[illegible]00*	12017,52	Augite	z	unresolved prob. no change
2700 region	12022,48	Pigeonite Augite	z	unresolved
2700	12018,50	Augite	z	unresolved

Effect of Heating at 200-225°C on Spin-allowed d-bands of Fe^{2+} in Lunar Rocks

	Rock No.	Mineral	Mineral Site	
~10,300A	10017,52	Augite	-	decrease
~ 9,900	10022,48	Pigeonite Augite	M_1	decrease
9,700	12018,65	Augite	M_1	decrease
9050	12018,65	Augite	M_1	decrease

* Cr^{3+} charge transfer band possibly also present.

activation energy then one at an M_2 site. These assignments are used later in Table 4.

The decrease in intensity of the Fe^{3+} bands is accompanied by decrease in intensity of two spin-allowed d-bands of Fe^{2+}, in rock 12018,65. These have both been assigned to the M_1 site (2). The two bands assigned to the M_2 site (2) show no change upon heating. The conclusion from this evidence is that only Fe^{2+} ions in sites preferred by Fe^{3+} have a charge transfer component in their spin-allowed d-transitions.

EXPERIMENTAL

The spectral data were taken using a Cary Model 14-R spectrophotometer with variable-voltage-halogen-lamp source for the visible and infrared spectral regions. Neutral density screens were used to obtain the high absorbance data in the ultraviolet region. The polarized spectra were taken using a calcite Glan prism that could be oriented to within ± 0.25°. Small circular matched slits were constructed in order to obtain the spectra of single crystals in the polished rock sections. The slits were individually made for each crystal investigated.

All rock sections were ∿30 microns thick, polished on both sides and mounted on brass holders containing the fixed slits. The polished sections had no backing so the thinness was limited to 30 microns in order to handle them without breakage. With this 30 micron thickness no sections were ever broken during the experiments. All heating experiments were performed on the thin sections without any mounting in order to avoid surface contamination. This necessitated replacement of the section in exactly the same position on the holder so that calculated difference spectra would be accurate. Replacement of minute single crystals exactly in the same position was difficult and difference spectra have as yet only been calculated using the spectrum of the whole rock, before and after radiation treatment.

Oscillator strengths of Fe^{3+} and Fe^{2+} bands in the pyroxene structure are unknown so that the Fe^{3+} concentrations are only order of magnitude estimates at best. It is considered that the total Fe^{3+} content is in the order of 0.0 X % by weight in the lunar rocks studied including Fe^{3+} in both tetrahedral and octahedral sites.

LOCATION OF TRANSITION CATIONS IN THE AUGITE STRUCTURE

Electron microprobe analyses across a zoned pyroxene crystal in section 12021,2 (7) show that in general as Si^{4+}, Mg^{2+}, Ca^{2+}, Al^{3+}, Ti, and Cr increase from pigeonite to augite the Fe^{2+} and Mn^{2+} decrease. From augite to pyroxferroite the trend reverses.

The lunar melt contains the 3d transition elements primarily in their lowest stable valence states namely Fe^{2+} ($3d^6$), Mn^{2+} ($3d^5$), Cr^{2+} ($3d^4$) and Ti^{3+} ($3d^1$). However titanium because of the stability of the unfilled 3d° configuration will partially be present as Ti^{4+}. Trace quantities of Fe^{3+} (ionic radius, r = 0.64A), and Cr^{3+} (0.63) present will follow Ti^{4+} (0.68) into the tetrahedral Si^{4+} (0.42) z- position along with Al^{3+} (0.52). As the tetrahedral Si^{4+} position in α-quartz can accommodate only cations differing by a charge of ± 1 (6), it is probable that this is also the case in the diopside structure of clinopyroxenes. Therefore one would not find Mg^{2+} (0.67), Fe^{2+} (0.74), or Mn^{2+} (0.80) in the tetrahedral site even if size consideration in case of Mg^{2+} would allow it. This conclusion is contrary to a suggestion of Verhoogen that Mg^{2+} may occupy a Si^{4+} site in clinoenstatite and diopside when titanium is present (8). Although Mg^{2+} may enter into tetrahedral coordination it is never found in the quartz structure, poor analytical data to the contrary. The ionic charge is too greatly different from the normal +4 in this cation position in the tetrahedral network. Thus in lunar pyroxene we are also undoubtedly limited to cations of +3 and +4 charge for silicon substitution in the chains of tetrahedra.

Since the original Ti^{3+} (0.76) in the lunar melt probably enters the M_1 site in augite, Al^{3+} is favored in the tetrahedral site for charge compensation. If one recalculates data of Dence et al (7) for number of atoms present one can compare the relative Al^{3+} to $Ti^{4+} + Cr^{3+}$ atom for atom. In their analysis number 4, for 503 x 10^{19} Si atoms there are 39 x 10^{19} Al, 9.5 x 10^{19} Ti and 8.0 x 10^{19} Cr atoms. If all the titanium were Ti^{4+} and Cr were Cr^{3+} and they occupied the M_1 site there would still be 12 x 10^{19} atoms of excess Al^{3+} if all went into the z site. This of course neglects possible trace Fe^{3+} in the M_1 and z sites from the original melt. Since there is Ti^{3+} and Cr^{2+} to be considered, and the Ti^{4+} that enters the z-site, it follows that there is Al^{3+} present in the M_1 site. If trace Fe^{3+} in the melt follows the Al^{3+} it will largely be present in the z site with possibly a smaller amount in the M_1 site.

As shown in Table 2 the three transitions assigned to Fe^{3+} in a tetrahedral site, $^4A_1{}^4E(G)$, $^4T_2(G)$ and $^4T_1(G)$ (9) are present in the lunar titanaugites, 12021,65 and 12018,50. The possible presence of tetrahedral Fe^{3+} in the Angra dos Reis meteoritic titanaugite and in lunar titanaugites indicates trace Fe^{3+} may have been present in the original melt. It was expected that a portion of the Fe^{3+} present may have entered the M_1 site. However octahedral transitions of Fe^{3+} seem absent in the lunar pyroxenes (except for possible charge transfer bands). Since Ti^{4+} is low in the pigeonite one would not expect much Fe^{3+} produced by radiation to occur, and Fe^{3+} would not tend to enter the z-site in this structure.

COMPARISON OF SPIN-FORBIDDEN TETRAHEDRAL BANDS OF Fe^{3+} IN TERRESTRIAL AND IN METEORITIC TITANAUGITE WITH THOSE IN TITANAUGITE IN ROCKS 12021,65 AND 12018,50.

Rock section 12021,65 is a coarse-grained porphyritic gabbro from Oceanus Procellarum and has zoned pyroxene phenocrysts as the major mineral. The complex

Table 2

Possible Transitions of Fe^{3+} in Tetrahedral Sites

Transition	Phlogopite(9)		Orthoclase(9)		Maui, Hawaii Augite		Angra dos Reis Augite	
	A	cm-1	A	cm-1	A	cm-1	A	cm-1
$^6A_1\rightarrow{}^4A_1{}^4E(G)$	4405	22700	3775	26500	α 4450 β 4470	23370	α,β 4500	22225
δcm^{-1}		2400		2500		1670		1825
$\rightarrow{}^4T_2(G)$	4925	20300	4165	24000	α,β 4855	20,600	α 4920 β 4900	20400
δcm^{-1}		1100		1350		1730		1370
$\rightarrow{}^4T_1(G)$	5210	19200	4415	22650	β 5300	18870	α 5210 β 5255	19030

Transition	Lunar Augite 12018,50		Lunar Augite 12021,65	
	A	cm^{-1}	A	cm^{-1}
$^6A_1\rightarrow{}^4A_1{}^4E(G)$	4550	21980	α,β 4500	22370
δcm^{-1}		1360		1750
$\rightarrow{}^4T_2(G)$	4850	20620	β 4850	20620
δcm^{-1}		1930		1750
$\rightarrow{}^4T_1(G)$	5350	18690	α 5250 β 5300	18870

nature of the pigeonite-augite phenocrysts has been described earlier (7, 10, 11). The crystal investigated here had a core ∿550 microns in diameter in the XY plane surrounded by a epitaxial zone of pigeonite-titanaugite with microscopically exolved augite lamellae observable in this zone. The absorption spectra of the pigeonite and titanaugite are shown in Figure 1. The possible Fe^{3+} tetrahedral spin-forbidden transitions are tabulated in Table 2. Absorbance values in Figure 1 are only approximate above 4.0ev (3100A) because of the intense absorption of the Fe^{3+} charge-transfer bands in the ultraviolet region. The anisotropy of the pigeonite was so small it was not studied in detail. Figure 2 gives the spectrum along the Y-axis, β = b and in the XY plane near α. The lunar titanaugite has too intense an absorption to be measured above 5.5 ev (∿2250A) in Figure 1 and the Glan Polarizer limits the polarized spectrum to 4.0 ev in the β spectrum in Figure 2. Figure 3 shows the spectral data of augite from lunar rock 12018,50 after heating and Figure 4 that for Angra dos Reis meteoritic augite. Lunar rock 12018 was recovered at Oceanus Procellarum by the Apollo 12 mission. It contains smaller crystals of pyroxene than in rock 12021 from the same mission and the transparent colored crystals are predominately titanaugite with some large crystals of olivine present. The rock is similar to a medium grained gabbro (12).

In Table 2 possible tetrahedral Fe^{3+} spin-forbidden transitions are listed for lunar augites in rocks 12018,50 and 12021,65. They are compared to data of Faye and Hogarth (9) on phlogopite and orthoclase and to data run in this laboratory on augite from Haleakala, Maui, Hawaii and augite from the Angra dos Reis meteorite. Chemical analyses for these augites with the exception of the one from rock 12018 are given in Table 3.

The Hawaiian augite with 3.36 Fe_2O_3 has a band at 4470A (β) as its most prominent band in the visible region. The band at 4855A is much less intense and the one at 5300A barely discernable. The latter is more pronounced in the Angra dos Reis augite spectrum. The absorbance decrease in these bands compares

Table 3

CHEMICAL ANALYSES OF TERRESTRIAL, METEORITIC, AND LUNAR PYROXENES

ELEMENT AS OXIDE	HALEAKALA, MAUI HAWAII (13)	ANGRA DOS REIS (14)*	TATAHOUINE (15)*	12021 LUNAR PIGEONITE (7)	12021 AUGITE(7)
SiO_2	47.70		53.7	51.5	50.2
Al_2O_3	6.82	21.5	0.45	2.05	3.32
Fe_2O_3	3.36				
FeO	4.43	8.4	13.89	16.9	13.1
MgO	13.34		28.2	21.9	15.3
CaO	21.35	∿ 23.8	0.72	5.1	15.7
Na_2O	0.65	0.08			
K_2O	0.03	0.012	—	—	—
TiO_2	1.89	2.8	0.03	0.68	1.26
Cr_2O_3	0.23	0.50	0.88	0.93	1.01
MnO	0.16	0.09	0.64	0.37	0.31
TOTALS	99.96		98.40	99.43	100.20

* whole meteorite analysis

favorably with those for the same transitions in phlogopite. The absorption bands in an unstrained tetrahedral position would be isotropic however the z-site in augite is somewhat distorted even though the distortion seems to decrease with substitution of Fe^{3+} (11). The bands are quite similar in the $\sim\alpha$ and β spectra although there are very slight wavelength shifts. The similarity of the $\sim\alpha$ and β spectra strengthen the probability that these are transitions of Fe^{3+} at a tetrahedral site. The presence of these bands in lunar augites strengthens the evidence for presence of Fe^{3+} in lunar minerals. Even though these assignments may turn out to be incorrect however it does not preclude the presence of Fe^{3+} in lunar augites as evidenced by the presence of charge transfer bands in the ultraviolet region.

There is a possibility that Fe^{2+} could occur at a z-site in the lunar augite as a result of radiation-reduction of Fe^{3+} located at this site. However the concentration would be low because of the small concentration of Fe^{3+} in the tetrahedral site.

Fe^{3+} CHARGE-TRANSFER BANDS IN LUNAR AND METEORITIC PYROXENES

Table 4 lists probable oxygen ligand - Fe^{3+} metal charge transfer bands in Angra dos Reis augite, lunar augite, lunar pigeonite and Tatahouine achondritic hypersthene in the ultraviolet region. Reasons for possible site assignments of the bands at 2700-2850A, 2600-2700A, and 2200A were discussed in the introduction.

The earlier work on whole rock spectra did not furnish the spectral resolution of this later work on single crystals, for this reason additional bands were detected in augite in lunar rocks 12018 and 12021 at 2450-2500A. The Angra dos Reis meteorite as shown in Figure 5 has all these bands as well as an additional one at 2400A not found in the lunar augite. The pigeonite-augite zoned-crystal in rock 12021 had too great an absorbance to measure the respective regions down to 2200A. This is also the case with the Tatahouine meteoritic hypersthene which has a cutoff at 2750A.

SPIN-FORBIDDEN Fe^{2+} BANDS IN THE VISIBLE REGION IN PYROXENES.

Table 5 lists possible bands assignments to spin-forbidden bands of Fe^{2+} in octahedral sites. Earlier assignments of the bands of enstatite in this region has been published by White and Keester (16). Burns and Huggins (17) assigned bands at 402, 425, 505, 550 and 585 nm. in zoned-pyroxenes in lunar rocks 10045, 10047, and 10058 to spin-forbidden transitions of Fe^{2+}. This work is in agreement with their assignments of these bands to spin-forbidden transition of Fe^{2+} as shown by the data in Table 5.

Mossbauer spectra of pyroxene in rock 12021 has been studied (18) and indicates that the subcalcic augite has 0.34 of the M_1 site occupied by Fe^{2+} and 0.52 of the M_2 site while the pigeonite has 0.12 Fe^{2+} in the M_1 site and 0.46 in the M_2 site. The bands at 5050 and 5500A in the pigeonite are most likely due to Fe^{2+} in an M_2 site.

CHARGE TRANSFER BANDS OF Fe^{2+} AND Ti^{3+}.

Table 6 lists bands at 6200A in augites that are probably due to $Fe^{2+} \rightarrow Fe^{3+}$ charge transfer. A band in this region in corundum has been discussed by Faye (19). The band in the region 4705-4800A is assigned to Ti^{3+} as a charge transfer band probably due to $Ti^{3+} \rightarrow Ti^{4+}$. It is probable that the Ti^{3+} is in the octahedral, M_1, position.

The Ti^{3+} band is most intense in the Angra dos Reis meteorite because of its high radiation age (20) and its high titanium content (14). Tatahouine hypersthene is so low in titanium that this band is absent. It is also weak in pigeonite where the titanium present may be largely due to exolved augite in the crystal.

Table 4

Fe^{3+} CHARGE TRANSFER BANDS IN THE ULTRAVIOLET SPECTRAL REGION IN SINGLE CRYSTALS

Possible Site	M_1	M_1(?)	M_2(?)	M_2	z
Specimen	λ in A	λ in A	λ in A	λ in A	λ in A
Angra dos Reis augite	2750	2500	2400	2200	2600
Lunar:					
12018,50 augite	2850	2500	-	2200	2700
12021,65 augite	2700	2450	-	?	2700
12021,65 pigeonite	2750	-	?	?	2600
Tatahouine hypersthene	2800	?	?	?	?

Table 5

SPIN-FORBIDDEN Fe^{2+} BANDS IN VISIBLE REGION IN PYROXENES

Transition $^5T_2(G) \rightarrow$	$^4A_1{}^4E(G)$	$^1T_1(G)$	$^1A_1(G)$
Specimen:	λ in A	λ in A	λ in A
Maui, Hawaii augite	β 4090	β 4250	α 5040 n 5040
Angra dos Reis augite	α 4050 β 4100	α 4295	α 5000 n 5000
Lunar:			
12018,50 augite	-	-	5065
12021,65 augite	-	β 4250	α 5050 β 5050 n 5050
12021,65 pigeonite	-	-	5050
Tatahouine hypersthene	4050	4250	5060

[illegible] = normal unpolarized light.

Transition $^5T_2(G) \rightarrow$	$^3T_1(G)$	$^4T_2(G)$
Specimen:	λ in A	λ in A
Maui, Hawaii augite	α 5400 β 5510 n 5450	β 5835 n 5805
Angra dos Reis augite	α 5585 β 5600 n 5550	α 5850 β 5890
Lunar:		
12018,50 augite	5500	5850
12021,65 augite	α 5650 β 5600 n 5500	α 5950 β 5950
12021,65 pigeonite	5500	-
Tatahouine hypersthene	-	-

n = normal unpolarized light.

Table 6

CHARGE TRANSFER BANDS OF $Fe^{2+} \rightarrow Fe^{3+}$ AND $Ti^{3+} \rightarrow Ti^{4+}$.

Specimen:	$Fe^{2+} \rightarrow Fe^{3+}$	$Ti^{3+} \rightarrow Ti^{4+}$
Maui, Hawaii augite	6200A	α 4705A β 4750
Angra dos Reis augite	α 6245 β 6200	α 4805 β {4750 4705
Lunar:		
12018,50 augite	6200	4700
12021,65 augite	β 6200	α 4750 β 4750 n 4800
12021,65 pigeonite	6400	4800
Tatahouine hypersthene	6000	–

n = normal unpolarized light.

OTHER ABSORPTION BANDS RELATED TO Fe^{3+} OR Fe^{2+} SPIN-FORBIDDEN TRANSITIONS.

Table 7 lists bands in the ultraviolet that are probably related to either Fe^{3+} or Fe^{2+} spin-forbidden transitions at an M site.

The terrestrial titanaugite had such intense absorption below 3700A that no data could be recorded.

Assignment of these bands will require further investigation. It is possible that a charge transfer component is present in several.

CONCLUSIONS

The presence of Fe^{3+} in terrestrial titanaugite is expected and shown by analytical means. Comparison of lunar and meteoritic titanaugite to the terrestrial mineral indicates bands that may be attributed to tetrahedral Fe^{3+} ion in all specimens. Evidence for the presence of Fe^{3+} in lunar and meteoritic pyroxenes is strengthened by the charge transfer bands in the ultraviolet region. The major Fe^{3+}-related charge transfer bands in the ultraviolet are attributed to M_1 and M_2 sites in the augite structure. The decrease of these bands on mild heating is evidence that a portion of Fe^{3+} in octahedral sites is produced by radiation probably cosmic rays acting on Fe^{2+}.

ACKNOWLEDGEMENTS

The author would like to especially thank Grover Moreland of the U. S. National Museum who made this work possible by his skillful preparation of the polished rock sections used in this work. The polished thin-section of the rare Angra dos Reis meteorite was obtained from the U. S. National Museum through the courtesy of Brian Mason. The Tatahouine achondrite was through the courtesy of J. Oscel, Museum National, d' Historie Naturelle, Paris, in 1959.

The writer acknowledges partial support from two NASA grants, NAS9-9942, and NGL39-011-085.

Table 7

POSSIBLE Fe^{3+} OR Fe^{2+} SPIN-FORBIDDEN ABSORPTION BANDS IN THE ULTRAVIOLET SPECTRAL REGION

Specimen:						
Maui, Hawaii augite	-	α 3750A	-	-	-	-
Angra dos Reis augite	3950A	3800	3350A	3250A	3100A	2950A
Lunar:						
12018,50 augite	-	-	3350	3250	3150	3000
12021,65 augite	-	-	-	-	-	3000
12021,65 pigeonite	-	-	-	-	-	-
Tatahouine hypersthene	-	-	-	-	-	2950

REFERENCES

(1) B. W. Hapke, A. J. Cohen, W. A. Cassidy and E. N. Wells, Science 167, 745-747 (1970).

(2) A. J. Cohen, International Astronomical Union Symposium No. 47 "The Moon" University of Newcastle Upon Tyne, March 1971, submitted for publication.

(3) B. W. Hapke, A. J. Cohen, W. A. Cassidy and E. N. Wells, Proceedings of the Apollo 11 Lunar Science Conference 3, 2199-2212, Pergamon Press (1970).

(4) A. J. Cohen and F. Hassan, Science 167, 176-177 (1970).

(5) S. S. Hafner and H. G. Huckenholz, Nature Physical Science 233, 9-10 (1971).

(6) A. J. Cohen and E. S. Hodge, J. Phys. Chem. Solids 7, 361-2 (1958).

(7) M. R. Dence, J. A. V. Douglas, A. G. Plant and R. J. Traill, Proceedings of the Second Lunar Science Conference, 1, 285-299, The M. I. T. Press (1971).

(8) J. Verhoogen, Amer. J. Sci. 260, 211-220 (1962).

(9) G. H. Faye and D. D. Hogarth, Can. Mineral. 10, 25-34 (1969).

(10) F. R. Boyd, Annual Report of the Director, Geophysical Laboratory, 1969-1970, Jan. 1971, pp. 216-228.

(11) S. S. Hafner, D. Virgo, D. Warburton, Nature Physical Science 231, 79-80 (1971).

(12) J. Warner, NASA Technical Report R-353 Dec. 1970 p. 90.

(13) H. S. Washington, Am. J. Sci., 3, 117 (1922).

(14) A. A. Smales et al, Science 167, 509-512 (1970).

(15) A. M. Reid and A. J. Cohen, Geochim. Cosmochim. Acta 31, 661-672 (1967).

(16) W. B. White and K. L. Keester, Am. Mineral 51, 774-791 (1966).

(17) R. G. Burns and F. E. Huggins, Lunar Science Institute Conference on Lunar Geophysics, Oct. 18-21, 1971, Houston, Abstract.

(18) L. S. Walter et al, Second Apollo Conference, Houston, Jan. 1971, preprint.

(19) G. N. Faye, Am. Mineral, 56, 344-348 (1971).

(20) R. Ganapathy and E. Anders, Geochim. Cosmochim. Acta 33, 775-789 (1969).

FIGURES

Figure 1. Lunar Rock, 12021,65, pigeonite core surrounded by overgrowth of augite, orientation of 30 micron thick section perpendicular to YZ plane. - - - - spectrum of pigeonite core, $\sim$550 microns diameter; ——— spectrum of augite overgrowth $\sim$250 microns wide.

Figure 2. Lunar Rock 12021,65. Polarized spectrum of augite zone. - - - - $b = \beta$; ——— in XY plane near α.

Figure 3. Lunar Rock 12018,50 after heating at 200-225°C for 2 hrs. absorption spectrum of single crystal of augite $\sim$400 microns diameter.

Figure 4. Polarized absorption spectrum of single crystal of augite from Angra dos Reis achondrite, crystal cut perpendicular to YZ plane. - - - - in XY plane near α; ——— $b = \beta$. Crystal 50 microns thick.

Figure 5. Absorption spectrum of same crystal as in Figure 4 in the ultraviolet region showing charge transfer bands of Fe^{3+}.

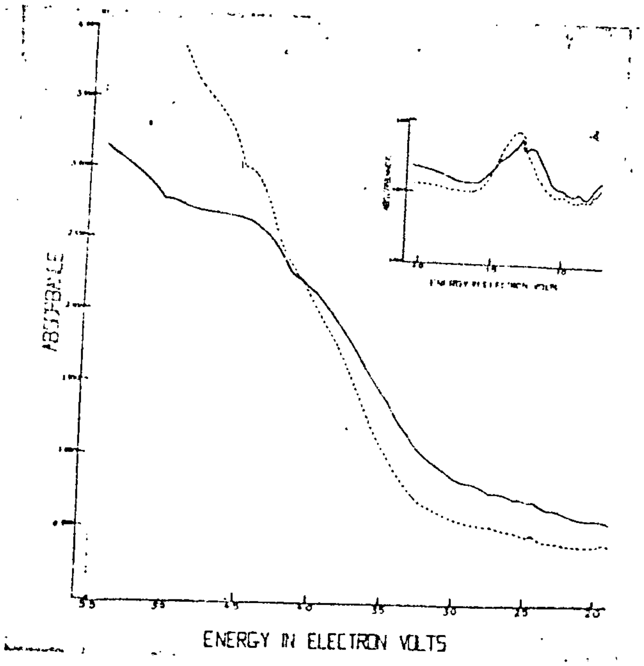

Figure 1

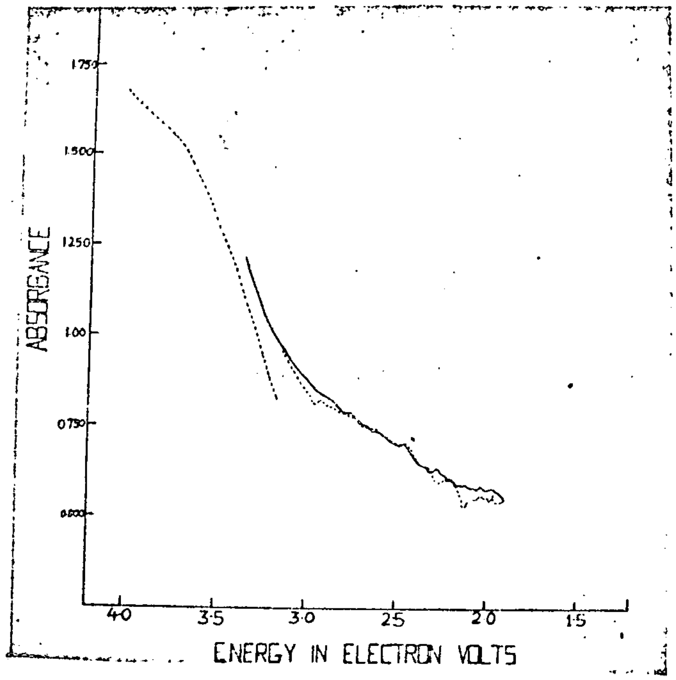

Figure 2

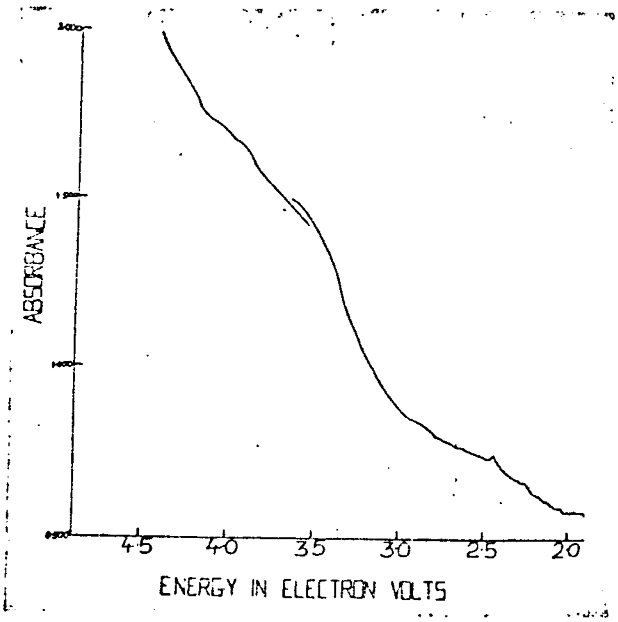

Figure 3

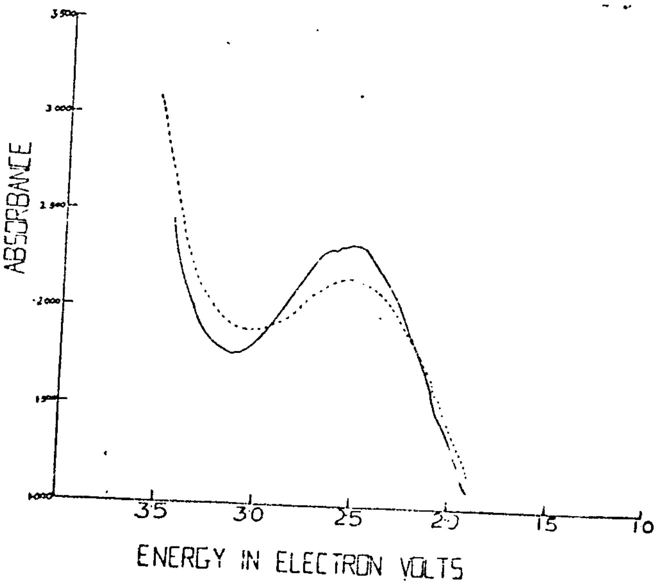

Figure 4

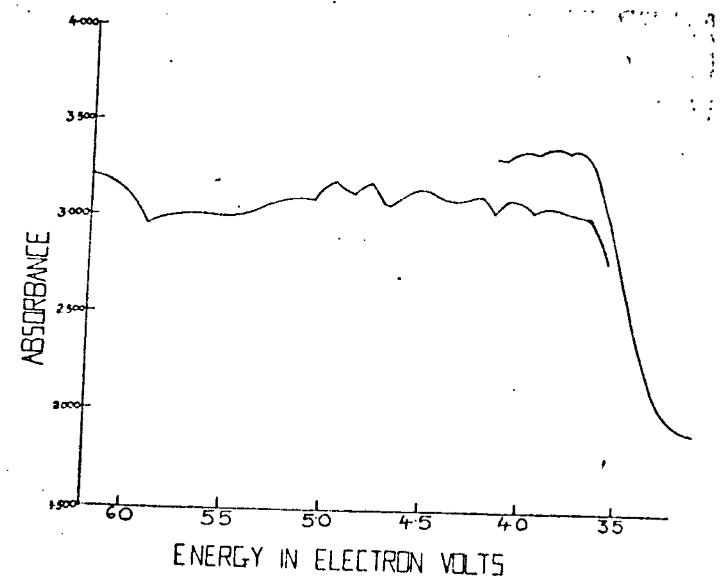

Figure 5

PROGRESS IN UNDERSTANDING THE OPTICAL SPECTRA OF LUNAR MATERIALS

B. Hapke, W. Cassidy, E. Wells
Department of Earth and Planetary Sciences
University of Pittsburgh
Pittsburgh, Pennsylvania 15213

This paper is a brief summary of results of research on the optical properties of natural and artificial lunar material accomplished since the Second Apollo Lunar Science Conference.

Spectra of Artificial Glasses

Serious differences exist in reports of spectra of glasses made from Apollo lunar crystaline rocks. Nash, Conel and Greer (1) and Adams and McCord (2) reported that such glasses have albedos and spectra similar to lunar soil. However, Hapke, Cassidy, and Wells (3) were unable to confirm these results.

It was suspected that these discrepancies might be due to differences in sample preparation. Though both groups used a nitrogen atmosphere, Nash, et al and Adams and McCord prepared their glasses by heating in a platinum crucible, while Hapke, et al prepared their samples in a graphite crucible. Accordingly, identical mixtures of powder were prepared using pure, reagent-grade oxides of SiO_2, Al_2O_3, CaO_2, FeO, MgO, and TiO_2 in Apollo 11 proportions. One mixture was heated to 1300°C in a platinum crucible and a second in graphite; in both cases the ambient atmosphere was dry, oil-free nitrogen gas. The resultant glasses were pulverized to 400f and their reflection spectra measured. These spectra are shown in Figure 1.

The platinum-prepared glass differs strongly from the graphite-prepared glass in having a lower albedo, having little trace of the Fe^{2+} band at 1μ and in having strong absorption in the 0.6-0.7μ range. The latter absorption is suspected to be due to charge transfer bands involving Fe^{3+}. The N_2 used was analyzed using a mass-spectrometer and was found to contain approximately 1,000 ppm of H_2O and O_2. Thus the conditions in the platinum crucible were, in fact, not neutral but slightly oxidizing, while those in the graphite crucible were reducing, since the hot carbon would keep the partial pressure of oxygen extremely low.

Although the spectrum of the platinum-melted glass more resembles the spectra of lunar soil than the graphite-melted glass, it is extremely doubtful if the platinum glass is representative of the glass in the lunar fines because of the oxidizing conditions necessary to produce it. It is highly likely that the glasses in the lunar fines were made under reducing conditions because of the metallic iron present in the fines and the low abundance of Fe^{3+}. The graphite-melted glass should be more similar in oxidation state to the lunar soil than the platinum-melted glass. However, since the graphite-melted glass possesses a prominent Fe^{2+} 1μ absorption band which is not present in the spectra of lunar soil, other processes must apparently be invoked to account for the spectra of the fines. We have previously suggested two processes, both of which involve deposition from a vapor phase: the vapor could be generated by either micrometeorite impacts or by solar-wind sputtering.

Solar Wind Irradiation

It has been suggested that sputtering by solar wind protons is a factor in the low albedo and characteristics spectrum of lunar soil. Extensive laboratory experiments have been carried out to back up this suggestion (4). However Nash (5) has critized these experiments on the grounds that the observed darkening of rock powders may be due to contamination by cracked diffusion pump oil or by iron sputtered from accelerator grids. Consequently, the irradiation has been repeated in an oil-free system evacuated by a sputter ion pump. In addition a magnetic deflector was used to separate the ion bean into its component species with differing charge-to-man ratios. Darkening by proton bombardment still occurred, confirming the original hypothesis.

Flash Evaporation

In order to crudely simulate the deposition of vapor from a meteorite impact, thin films were made by flash evaporation of lunar crystalline rock material coating a tungsten filament. Although such films were highly absorbing and had the correct optical properties to account for the lunar spectrum, electron microprobe analyses showed that the films were heavily contaminated with tungsten. Consequently, films which are believed to be free of tungsten havebeen formed by evaporating basaltic-rock powder in an electron-beam furnace. In this apparatus the tungsten filament is completely shielded from the evaporant and the substrate. These films are presently being analyzed; their optical properties appear to be qualitatively similar to fims formed by flashing from a tungsten filament. Thus the hypothesis of darkening by deposition of vapor appears also to be confirmed.

References

1. D. Nash, J. Conel and R. Greer, Science, 167, 7 1 (1970).
2. J. Adams and T. McCord, Proc. Second Lunar Sci. Conf., 2183 (1971).
3. B. Hapke, W. Cassidy and E. Wells, paper presented at Second Lunar Sci. Conf. (1971).
4. B. Hapke, Science, 159, 76 (1968).
5. D. Nash, J. Geophys. Res., 72, 3089 (1967).

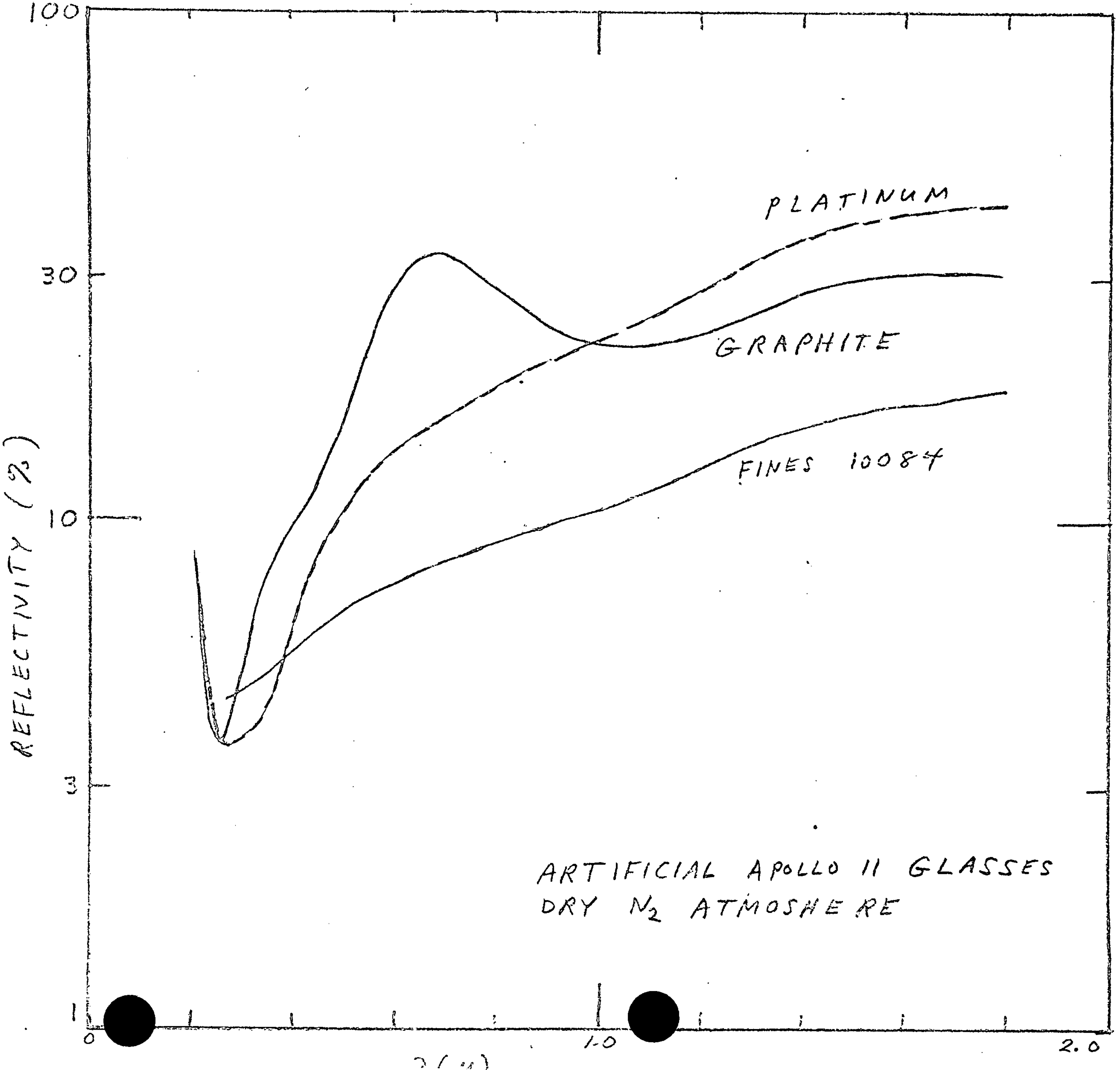
PLATINUM
GRAPHITE
FINES 10084
ARTIFICIAL APOLLO 11 GLASSES
DRY N_2 ATMOSHERE
REFLECTIVITY (%)
100
30
10
3
1
0
1.0
2.0
λ(μ)

Radiation Effects in Lunar Crystalline Rocks

Summary of Work

by

Alvin J. Cohen
University of Pittsburgh

All lunar rocks studies contained light brown pyroxenes of at least two varieties. All color changes due to ultra-violet and X-ray radiation, found by light transmission studies, are related to changes in these minerals. The ilmenite is opaque and the plagioclase is inert to radiation damage at low energies, because of its purity, when formed under reducing conditions (Ref. 1).

Olivines are low in 10017 and 10022 and no changes were observed in preliminary work in 12018 except a Fe^{2+} band splitting not seen in 10017 and 10022, probably due to Fe^{2+} in the olivine.

Heating experiments give similar results in Apollo 11 and 12 crystalline rocks. All rocks show reduction of original Fe^{3+} present in the pristine rock when heated above 200° C. in air. The following reaction takes place, as shown by changes in absorption spectra:

$$Fe^{3+} \text{ (trace)} + Cr^{3+} + Ti^{3+} \rightarrow Fe^{2+} + Cr^{2+} + Ti^{4+} \quad (1)$$

In 12018 there was no change on heating at 140° C, 150° C, 175° C. and 198° C., for several hours in each case. Heating at 200-225° C for two hours resulted in reaction (1).

It may be concluded that heating to this temperature, as by a very large solar flare, would cause the lunar surface to lighten. This reaction may be reversed by treatment with UV and visible light from a Xenon-Mercury lamp:

$$Fe^{2+} + Ti^{4} \xrightarrow{UV} Fe^{3+} \text{ (trace)} + Ti^{3+} \quad (2).$$

Due to the high oscillator strength of Fe^{3+}, p.p.m. abundances cause observable lightening or darkening of the lunar rock depending on oxidation or reduction of trace Fe^{3+} originally present in the pristine lunar pyroxenes. The solid state reactions seem complex, involving Fe^{3+}, Fe^{2+} possibly Fe^{1+}, Ti^{4+}, Ti^{3+} Cr^{3+}, Cr^{2+} and possibly Mn^{3+}, and Mn^{2+} in the pyroxene sites. The mechanisms can be better understood by solid state work on terrestrial analogues of similar structure (Ref. 2).

The light lunar surface layer may be related to changes in the pyroxene Fe^{3+} content in crystalline rock fragments not coated with opaque matter. The percentage of this mater-al in lunar soil was not determined in this part of the study. The mechanisms found are those predicted in this laboratory in 1968 based on earlier work of Hassan and Cohen (Ref. 4).

REFERENCES

(1) a. Solar Radiation Effects on the Optical Properties of Apollo 11 Samples, B. W. Hapke, A. J. Cohen, W. A. Cassidy, and E. N. Wells, Proceedings of the Apollo 11 Lunar Science Conference Vol. 3, pp. 2199 to 2212 (1970).

b. Solar Radiation Effects in Lunar Samples, Ibid., Science <u>167</u>, 745-747 (1970)

(2) Iron in Synthetic Quartz: Heat and Radiation Induced Changes, A. J. Cohen and F. Hassan, Science <u>167</u>, 176-177 (1970)

(3) Radiation Bleaching of Thin Lunar Surface Layer, A. J. Cohen and B. W. Hapke, Science <u>161</u>, 1237 (1968).

(4) F. Hassan and A. J. Cohen (In preparation).

THE ALBEDO OF THE MOON: EVIDENCE FOR VAPOR-PHASE DEPOSITION PROCESSES ON THE LUNAR SURFACE

by

B. W. Hapke, W. A. Cassidy, and E. N. Wells

University of Pittsburgh

I. INTRODUCTION

Ever since the optical properties of the lunar surface have been understood semi-quantitatively, the low albedo and reddish spectrum of the moon have seemed puzzling. Various hypotheses suggested to account for the low albedo of the lunar soil include the following: (1) the lunar material is intrinsically dark, (2) lunar soil grains are coated by hydrocarbons or other dark volatile material outgassed from the interior, or (3) lunar surface material is darkened by shock effects associated with meteorite impacts, or (4) some form of radiation damage (1, 2, 3). From a variety of earth-based observations, such as that recent impact features generally have high albedos, it has been concluded that the low albedo of the moon is due to an external darkening process whose effects may be modified by composition. The primary purpose of our investigation of lunar samples has been the understanding of this darkening process. We believe that the optical properties of the moon point strongly to vapor-phase deposition as an important process on the lunar surface.

II. OPTICAL PROPERTIES OF LUNAR ROCKS AND FINES

The reflection spectrum of the fines of Apollo 11 are shown in Fig. 1. This spectrum is characterized by a low albedo in the visible, a reflectivity which increases monotonically with wavelength, an extremely weak absorption band at 1 μ, which is believed to be due to ferrous ions in silicate, but with no sign of absorption bands in the vicinity of 0.5 μ or 0.3 μ. The spectrum of the Apollo 12 surface fines is also shown in Fig. 1, and is similar, except for a somewhat higher albedo and enhanced ferrous band. By contrast, the spectra of lunar crystalline rocks (Fig. 2) pulverized to the same degree of fineness as the soil are characterized by an albedo almost twice as high as that of the fines, a spectrum which is relatively flat above 0.4 μ, a pronounced absorption band in the ferrous position at 1 μ, and weak bands at 0.5 μ and 0.3 μ. We tentatively identify these latter bands as due to Ti^{+3} and Cr^{+3}, respectively.

According to most models for the origin of the lunar regolith, most of the fines are probably local in origin and come from within a few kilometers of their present location (4). Also, for the Apollo 11 samples, the crystalline rocks and the fines are very similar in composition. Thus it is likely that the parent material of the bulk of the Tranquility Base fines is similar to the Apollo 11 crystalline rocks. The situation is less clear for the relationship between Apollo 12 rocks and fines because, apparently, the Apollo 12 area is a much more geologically complex region. However, it appears clear that lunar crustal rocks are not intrinsically dark.

It seems reasonable to assume that the primary parent material of the fines is similar to the lunar crystalline rocks and is not some unknown, esoteric substance. Thus, whatever darkening process is acting on the lunar surface must have the capability of altering the optical properties of impact-pulverized lunar crystalline rocks to those of the lunar fines. This process must clearly be externally controlled and also must be able to operate on a small scale as well as a large scale. Given enough time, the process must be capable of darkening the ejecta of a crater a few tens of meters across as well as ray systems hundreds of kilometers in diameter, so that eventually the ray material will be optically indistinguishable from the detritis upon which it was deposited.

III. EVIDENCE FROM ANALYSES OF LUNAR MATERIAL FOR THE NATURE OF THE DARKENING PROCESS

1. Volatile coatings

No evidence was discovered for any sort of coatings on the lunar fines by material volatile at low temperatures. The fines were heated in a vacuum of 1 x 10^{-7} torr to 900°C (slightly below the sintering temperature) with no increase in albedo. Thermo-gravimetric analysis of a sample of fines in N_2 showed no loss of weight at any temperature below 900°C. It has been shown (5, 6) that a dark component of the fines is soluble in dilute HCl; our analysis (Table 1) of the leached material showed it to contain primarily the same major cations as the lunar crystalline rocks.

2. Matrix material of the microbreccias.

Microscopic examination of the fines by ourselves and others (7-13) disclosed that most of the dark particles in the lunar fines are either fragments of poorly transmitting glass or are microbreccia particles consisting of crystals and glass of varying degrees of transparency cemented together by a highly-absorbing, dark, amorphous matrix material, which is opaque in thicknesses greater than a few microns. Thus the problem of the darkening process appears to be related to the nature of the dark matrix material. This glass is a coating in the sense that, as a cementing medium, it envelopes the grains.

In order to study the matrix material further, a series of leaching experiments on the various lunar materials were carried out using 20% HCl at room temperature for one hour. Weight loss by acid treatment was measured, and the leach solution analysed by spark-emission spectrography. The results are shown in Tables 1 and 2. The lunar fines and breccia were readily attacked by the acid, losing as much as 25% of their weight. However, the crystalline rocks were much less affected. The albedo of the fines increased greatly upon leaching, and the spectral bands become more pronounced, as shown in Fig. 3. Among the various Apollo 11 and 12 fines, albedo was directly correlated with weight loss by acid-leaching: the darker the original material, the greater its weight loss upon leaching.

The leach solutions contained all the common cations of the crystalline rocks, implying that the increase in albedo is not simply the result of removing surface deposits of meteoritic nickel/iron.

Monitoring the leaching process under the microscope showed that as the apparently opaque particles were attacked by the acid, the dark matrix material dissolved; the grains lightened, and progressively disaggregated, leaving minute, transparent SiO$_2$-rich, grains of material as a residue. The reactivity of this matrix material may be due to strain and/or high defect densities. Samples of Apollo 11 fines which had been annealed in vacuum at 900°C showed negligible susceptibility to leaching (Table 2), which suggests that strains and defects had been annealed out.

3. The problem of the opacity of the amorphous matrix material

Agrell et al (7) and Chao et al (13) discovered myriads of tiny inclusions in portions of the glass in the lunar fines which they assume to be meteoritic nickel/iron. Thus the glass may be opaque because of Rayleigh absorption by the metallic micro-inclusions. However, as shown in Table 1, the leached solution contains only very small quantities of nickel. By inference, the amount of meteoritic nickel/iron removed from the fines by acid treatment is very low and cannot account for the opacity of the matrix glass.

Nash et al (14) suggested that the low lunar albedo is due primarily to the abundant glass in the fines. To support this conclusion they showed in their paper a spectrum of vitrified crystalline Apollo 11 rock, which indeed has an albedo much lower than before melting. We conducted a series of experiments in which an Apollo 11 crystalline rock was successively heated to various temperatures ranging from below the solidus temperature to well above the liquidus. The heating was done in a nitrogen atmosphere using a graphite crucible; thus the conditions were reducing. Following each heating the sample was rapidly quenched by immersion in liquid N_2. It was then pulverized to finer than 37 microns and its spectrum and albedo measured. The results are shown in Fig. 4. The darkening of the rock is pronounced, possibly due to diffusion of Fe and Ti. However, the spectrum of the vitrified rock clearly does not resemble the spectrum of the fines at any temperature. In particular, as the temperature nears liquidus point, the one micron band in the quenched material becomes very prominent. By contrast, it is clear that the spectrum of the fines requires a component which has no absorption band at all in the region of *one* micron. Clearly, a glass which is quenched from a melted crystalline rock cannot be invoked to account for the low lunar albedo and smooth spectrum.

Another possibility is that the dark matrix material may have been vapor-deposited. The source of this vapor may be sputtering by the solar wind (15) and/or vaporization by meteorite impact (5). In order to assess these possibilities thin films were prepared from Apollo 11 crystalline rocks by two processes. A sample was irradiated with 2 kilovolt hydrogen ions to simulate the solar-wind effect on the lunar surface. It has been previously reported (5, 15, 16) that such a process will darken pulverized crystalline rock. In this experiment a plate of fused silica was held near the target in such a way as to collect atoms sputtered from the rock. Second, in order to simulate crudely the process of vaporization by meteorite impact a sample of crystalline rock was pulverized to a fine powder and placed in a vacuum system. A tungsten filament was arranged so that it could be dipped into the powder, lifted up, and momentarily heated by passing a current through it. This process was repeated several times, and a portion of the vaporized material collected on a fused silica plate.

The spectra of these films are shown in Fig. 5. Even though these materials contain abundant Fe^{+2} ions there is no sign of any absorption bands in the transmission spectra. The films are transparent in the infra-red, but absorbing in the visible and ultra-violet and have optical densities greater than 1000 cm^{-1} in the visible. Spectra of lunar materials coated with flash-evaporated films are shown in Fig. 2. Contamination of the films by tungsten from the filament may be significant; nevertheless, these spectra are qualitatively similar to those of the fines.

The films have a low electrical conductivity and thus are not metallic. We believe that the reason films deposited in such a manner have a high opacity is that they are non-stoichiometric, being deficient in oxygen (15). It is well known from experimental thin film work (17) that when a film of a multi-component material, whose elements have very different vapor pressures and sticking coefficients, is deposited in a hard vacuum, non-stoichiometry almost invariably results. The oxygen deficiency probably allows absorption of light by electron-transfer processes. (Many common materials, such as ferrous oxide and titanium dioxide, are often opaque because of electron-transfer absorption related ~~due~~ to non-stoichiometry). When a vapor-deposited absorbing film was heated in air to 500°C its transparency increased markedly, presumably due to uptake of oxygen.

There is considerable evidence that the lunar fines are similarly deficient in oxygen. Ehmann and Morgan (18) measured the oxygen abundance of the fines and find an apparent depletion of oxygen. We heated a sample of Apollo 11 fines ~~was heated~~ in air to successively higher temperatures up to 900°C. Following each heating the spectrum and albedo of the sample were measured. These spectra are shown in Fig. 6. Very little change occurred in the spectrum of the fines until a temperature of about 500°C was reached. At this temperature the spectrum became redder and the ferrous ion band became more pronounced, even though the heating was being done under highly oxidizing conditions. It was not until a temperature of 900°C was reached that the 1 μ ferrous band began to disappear. We interpret the lower-temperature changes as due to the diffusion of oxygen into the non-stoichiometric material in the lunar fines, causing the formerly opaque matrix to become transparent and disclosing the ferrous band in the underlying minerals. Apparently the ferrous ions in the lunar fines themselves do not become oxidized to ferric ions until temperatures of nearly 900°C. are reached.

Thermo-gravimetric analyses were carried out in an oxygen atmosphere to 1100°C. The fines increased their weight by about 2%, whereas a sample of pulverized crystalline rock gained only 1%. If all iron in the samples, according to the published analyses, were oxidized to ferric iron, the weight gain due to the uptake of oxygen would be approximately 1%. The excess weight gain could well have been due to uptake of oxygen as the films moved toward stoichiometry.

IV. CONCLUSIONS

The low albedo of the moon, its reddish spectrum, and the lack of ferrous bands appear to be caused by a glassy matrix material in the fines. Although much of the lunar glass probably has not been condensed from a vapor, it does not seem possible to explain the optical properties of the amorphous matrix material except by deposition from a vapor-phase. Because of the close association of this material with shock and its apparent connection with meteorite impact, the most probable source of the vapor is vaporization of lunar material by meteorite impacts. However, sputtering by the solar wind may be a secondary source.

The impacting objects responsible for the glassy matrix material are most probably in the millimeter to centimeter range, rather than much larger objects. Large impact craters and their associated ejecta patterns have high albedos rather than low. Chao et al (13) find little evidence for cation fractionation in the lunar glass. Thus, the trajectories of the atoms during deposition are probably line-of-sight, as would be the case for small impact events, rather than diffusion of vapor, as in the large base-surge cloud discussed by McKay (10).

V. ACKNOWLEDGMENTS

We thank the following persons for their assistance: E. Hodge, E. Skopinski, J. Annania, M. Haller and F. LaPlante. We especially thank G. Aubele and the Fisher Scientific Company for their cooperation. This research was supported by NASA contract NAS 9-9942.

VI. REFERENCES

1. B. Hapke and H. Van Horn, J. Geophys. Res., <u>68</u>, 4545 (1963).
2. B. Hapke, Radio Sci., <u>5</u>, 293 (1970).
3. T. Gold, Mon. Not. Roy. Astron. Soc., <u>115</u>, 585 (1955).
4. E. Shoemaker, et al., Geochim. et Cosmochim. Acta, Suppl. 1, (1970), p. 2399.
5. B. Hapke, et al., Ibid., p. 2199.
6. T. Gold, et al., Ibid., p. 2149.
7. S. Agrell, et al., Ibid., p. 93.
8. M. Duke, et al., Ibid., p. 347.
9. C. Frondel, et al., Ibid., p. 445.
10. D. McKay, et al., Ibid., p. 673
11. J. Smith, et al., Ibid., p. 897.
12. J. Wood, et al., Ibid., p. 965.
13. E. Chao., et al., J. Geophys, Res., <u>75</u>, 7445 (1970).
14. J. Conel and D. Nash, Geochim. et Cosmochim. Acta, Suppl. 1, (1970), p. 2013.
15. B. Hapke, Ann. N. Y. Acad. Sci., <u>123</u>, 711 (1965).
16. B. Hapke, Science, <u>159</u>, 76 (1968).
17. L. Holland, <u>Vacuum Deposition of Thin Films</u>, New York, Wiley (1956).
18. W. Ehmann and J. Morgan, Geochim. et Cosmochim. Acta, Suppl. 1, (1970), p. 1071.

TABLE I.

SELECTED SPARK-EMISSION SPECTROGRAPHIC ANALYSES OF MATERIAL LEACHED FROM APOLLO 11 SAMPLES

(μg leached/mg of sample)

Si	Al	Fe	Mg	Ca	Na	K	Ti	Ni	TOTAL	
1	2	3.5	0.2	2.4	0.2	nd	0.7	nd	10.0	(1)
20	23	22	15	28	0.3	nd	25	0.6	133.9	(2)
45	42	56	76	57	0.7	2	74	0.8	371.5	(3)

(1) CRYSTALLINE ROCK 10017,52
(2) FINES 10084
(3) BRECCIA 10065,29

TABLE 2

WEIGHT LOSS BY ACID-LEACHING

(20% HCl for 1 hour; corrected for handling losses.)

MATERIAL	WEIGHT LOSS
SURFACE FINES 10084,81	10 ± 2%
VACUUM-ANNEALED FINES 10084,81	0
BRECCIA 10048,44	25
CRYSTALLINE ROCK 10017,52	4
VITRIFIED ROCK 10017,53	10
SURFACE FINES 12001,51	6
TRENCH FINES 12037,62	1

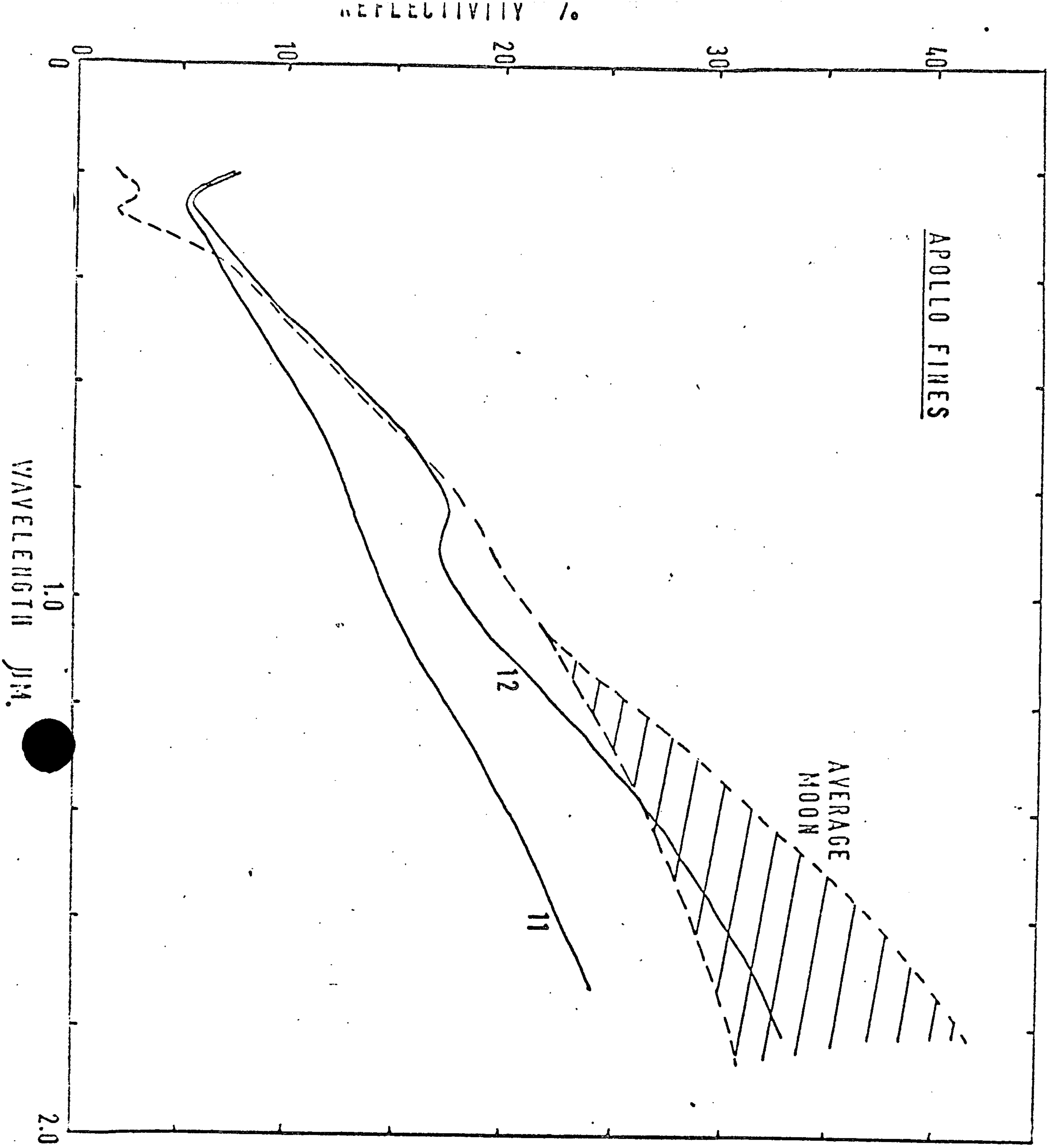

Fig. 1. Reflection spectra of Apollo 11 and 12 surface fines, compared with the integrated spectrum of the moon.

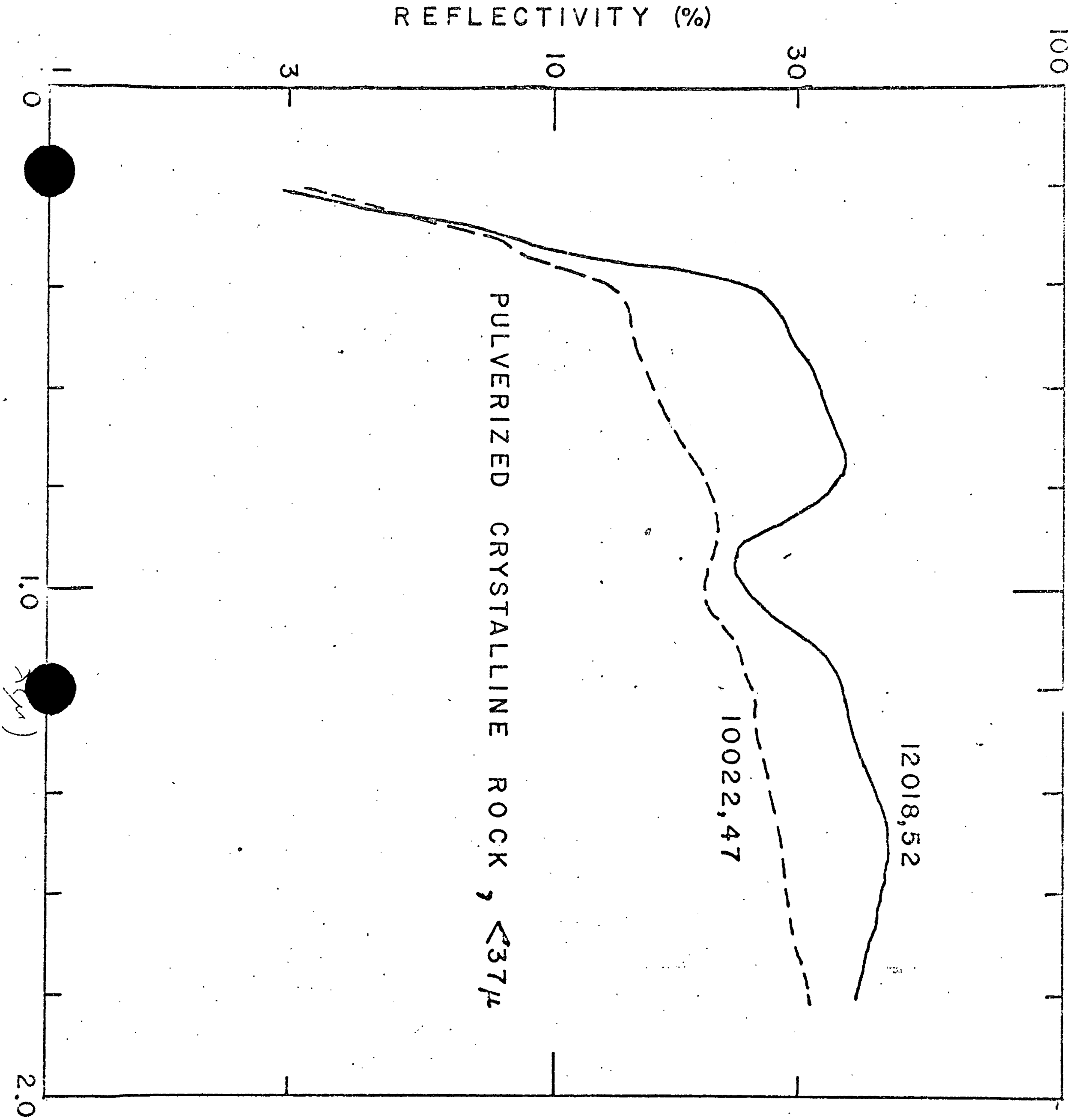

Fig. 2. Reflection spectra of Apollo 11 and 12 samples of crystalline rock, pulverized to finer than 37μ.

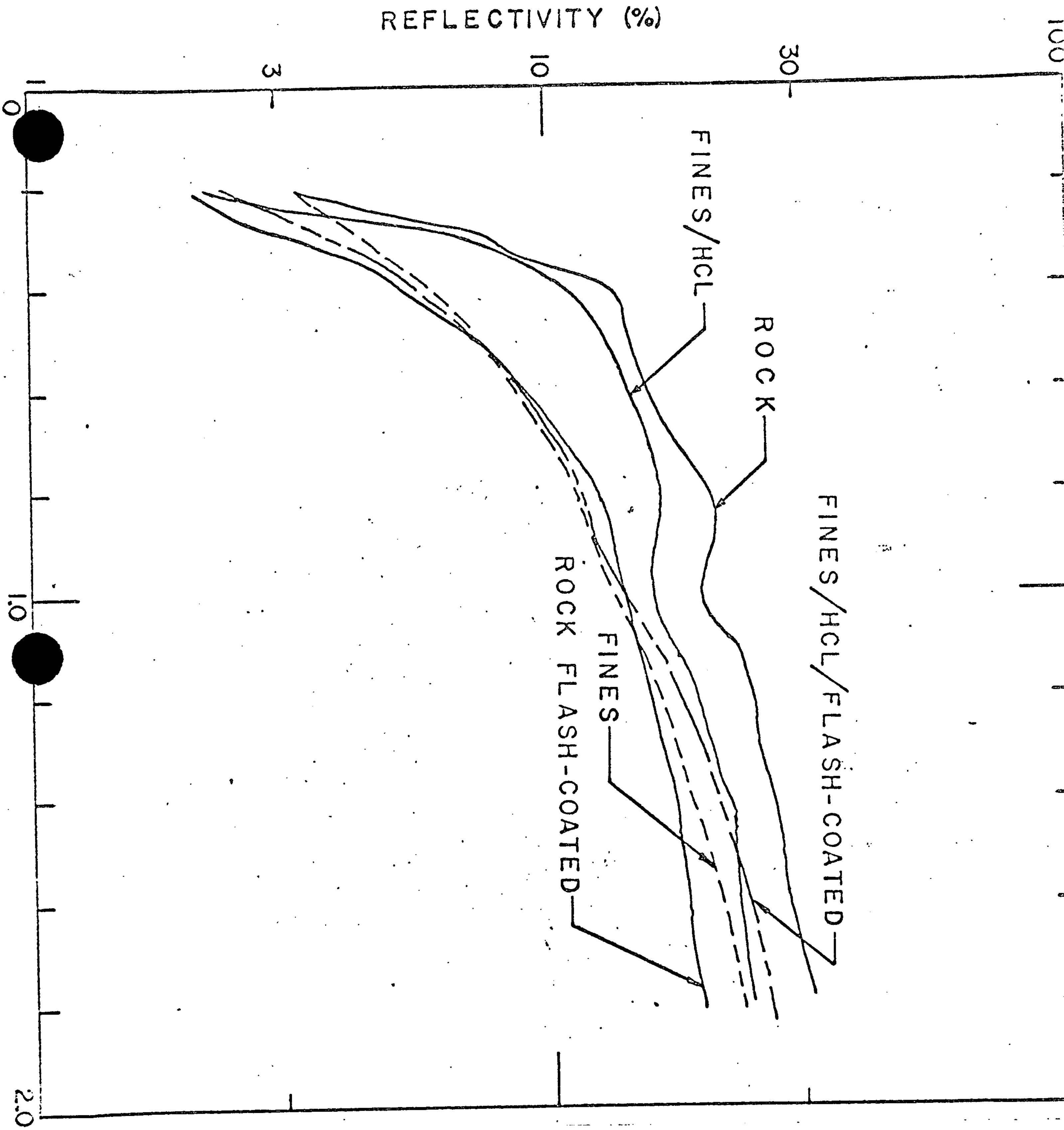

Fig. 3. Reflection spectra of Apollo 11 lunar material. Rock: crystalline rock 10017, pulverized to finer than 37μ; Fines: untreated fines 10084; Fines/HCl: residue of fines after treatment for 1 hour with 20% HCl; Fines/HCl/Flash-coated: acid-treated fines coated with the same material flash-evaporated from a tungsten filament; Rock/Flash-coated: powdered rock coated with the same material flash-evaporated from a tungsten filament.

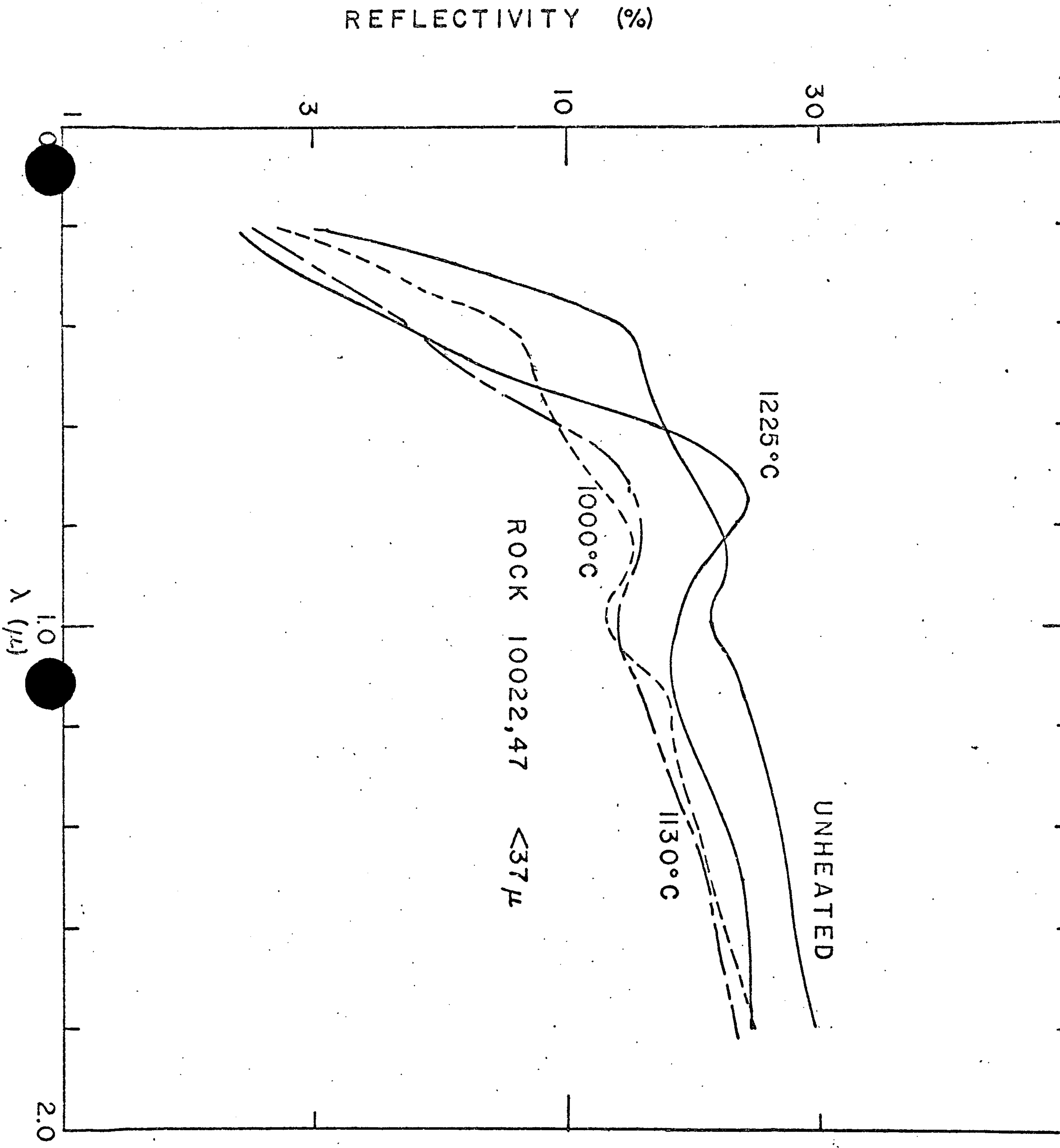

Fig. 4. Reflection spectra of Apollo 11 crystalline rock 10022 heated in a graphite crucible in N_2 to the designated temperature and rapidly quenched.

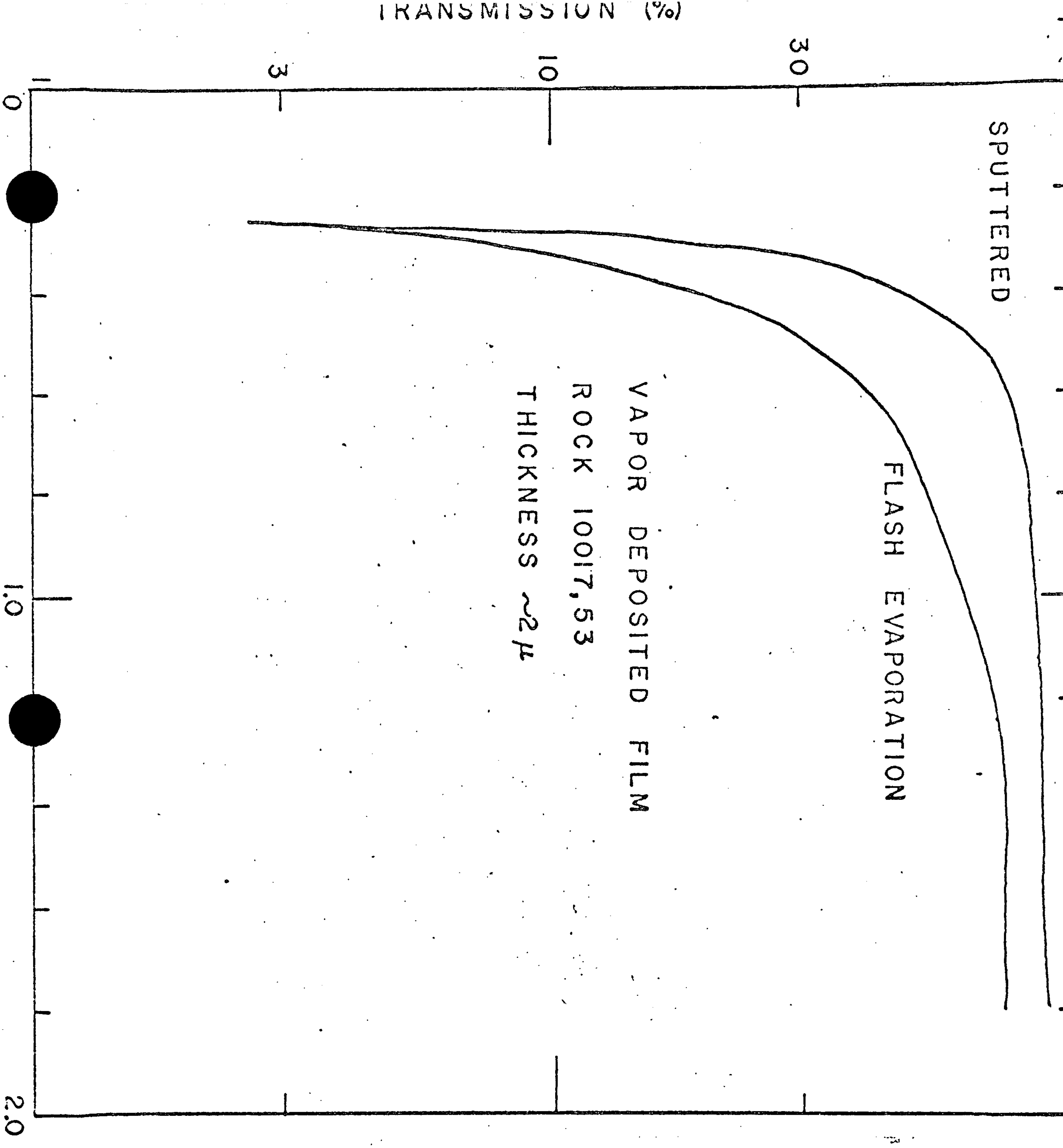

Fig. 5. Transmission spectra of thin films of Apollo 11 crystalline material prepared by sputtering by 2 kev hydrogen ions and by flash-evaporation from a tungsten filament.

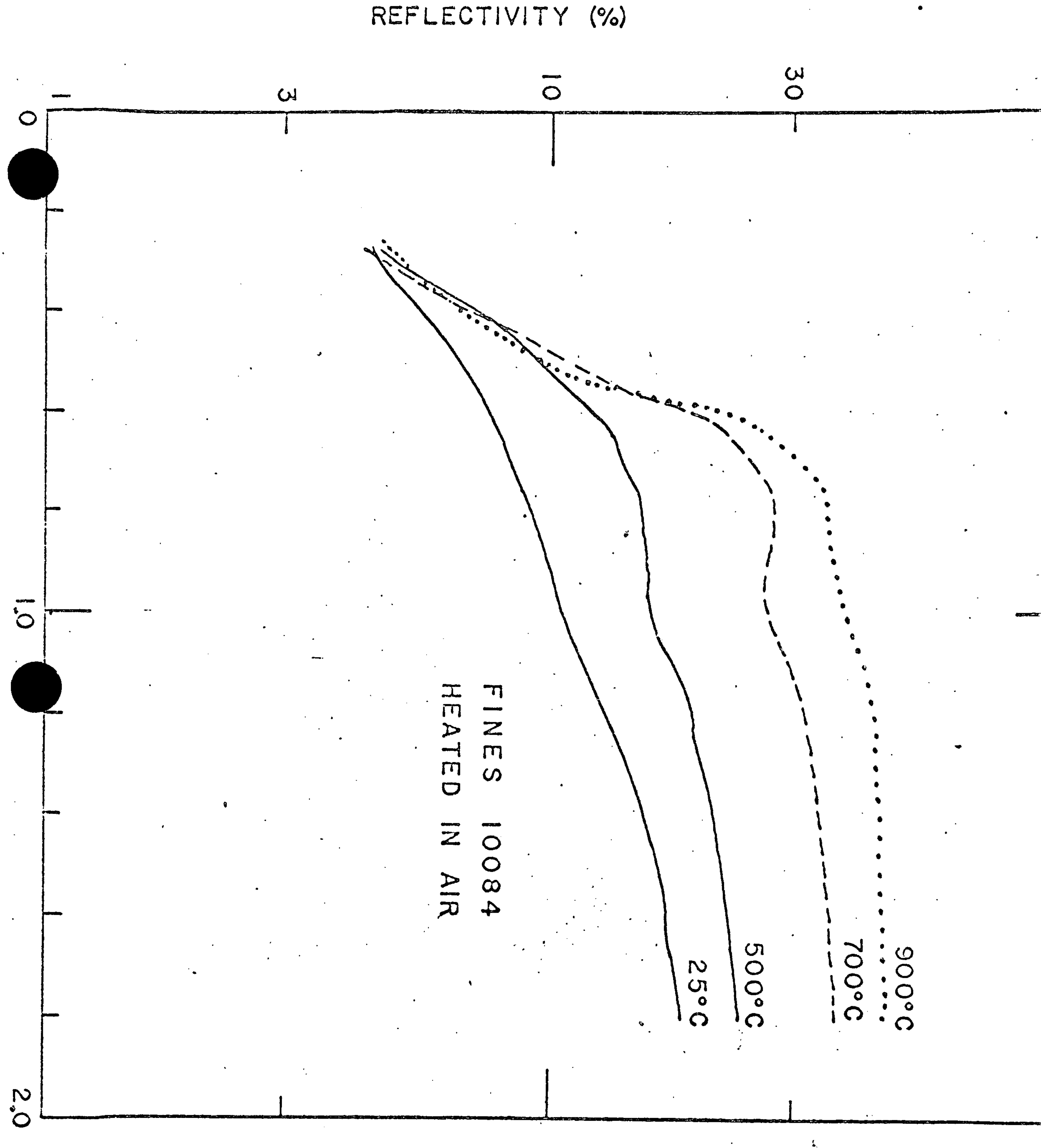

Fig. 6. Reflection spectra of Apollo 11 fines heated in air to the designated temperature for 2 hours.

INTERNATIONAL ASTRONOMICAL UNION
SYMPOSIUM NO. 47
"THE MOON"
UNIVERSITY OF NEWCASTLE UPON TYNE
22-26 MARCH 1971

THE VALENCE STATES OF 3d - TRANSITION ELEMENTS IN APOLLO 11 AND 12 ROCKS

BY ALVIN J. COHEN
DEPARTMENT OF EARTH AND PLANETARY SCIENCES
UNIVERSITY OF PITTSBURGH
PITTSBURGH, PA. 15213 U.S.A.

ABSTRACT

The absorption spectra of Apollo 11 fine-grained rocks, 10017 and 10022 are due entirely to pyroxene minerals. Spectral bands due to Fe^{3+}, Fe^{2+}, Cr^{3+} and Ti^{4+} and Ti^{3+} are detected. Single crystals of olivine in rocks 12021 and 12018 show bands due to Fe^{3+}, Fe^{2+}, Cr^{3+}, Ti^{3+}, Mn^{3+}, and Mn^{2+}. Pyroxenes in the same rocks exhibit band maxima of the same cationic species as in the olivines. Spectral shifts are noted due to anisotrophy of the crystal structures.

Heating sections 10017, 10022, and 12018 from the rock interiors at 200-225°C for 2 hours caused large decreases in the spectral intensity of Fe^{3+}, Cr^{3+} and Ti^{3+}, indicating the following reaction:

$$Fe^{3+} + Cr^{3+} + Ti^{3+} \rightarrow Fe^{2+} + Cr^{2+} + Ti^{4+}$$

This suggests that Fe^{3+}, Cr^{3+} and (a portion of) Ti^{3+} are not in equilibrium. It is most probable that they were produced subsequent to the formation of the rocks by a combination of secondary ionization processes following cosmic ray bombardment and by trace radioactivity present in the rocks.

An orange glass, 150 microns in diameter and 50 microns thick contained in brecciated rock, 10048,44, exhibited 15 identifiable absorption bands related to Fe^{2+}, Cr^{3+}, Ti^{3+}, Mn^{3+} or Mn^{2+} ions.

Plagioclase in 12021,65 has perfect transmission over the region studied. The limit of Fe^{3+} is in the order of <1 ppm and Fe^{2+}, 1000 ppm or less in this plagioclase single crystal of dimensions 0.6 mm x 0.2 mm x 30μ.

INTRODUCTION

Although Fe^{3+} and Ti^{3+} have been detected in Apollo 11 rocks by spectrophotometric (Hapke, Cohen, Cassidy and Wells, 1970) and by EPR techniques (Weeks, Kolopus, Kline and Chatelain, 1970), no mechanism for their origin in lunar minerals has hitherto been suggested. The absorption spectra of lunar pyroxene and olivine crystals are reported here in detail for the first time. Due to the random orientation of these crystals, in polished sections 30 microns thick, the anisotropy of the spectra was not investigated.

EXPERIMENTAL

The absorption spectral data were taken using a Cary Model 14 Spectrophotometer with IR - 1 Modification and a halogen lamp of variable intensity as a light source in the visible and infra-red regions investigated. The spectra of the small single crystals and glass were measured using matched circular slits of 2 mm diameter in sample and reference beams of the instrument. All samples investigated were approximately 30 microns thick except for the orange glass from rock 10048,44 which was approximately 50 microns thick. All single crystals measured were 2 mm or greater in diameter except the pyroxene, 12018,50 which was a grouping of several smaller crystals. The orange glass was 150 microns in diameter, surrounded by an opaque matrix of the breccia in which it was embedded.

The thinness of the specimens studied precluded detection of weak d-d transitions of the Fe^{3+} ion. The 30 micron thickness was necessary in order to study the intense Fe^{3+} charge-transfer bands in the ultraviolet region. The Fe^{3+} band peak could not be measured in the orange glass due to the thickness of 50 microns. Screens were used in the reference beam to extend the optical density range of the spectrophotometer in order to measure the Fe^{3+} peak in all cases.

The polished sections were mounted on specially machined brass holders so that the spectrophotometer beam passed only through the sample under investigation, no other extraneous matter being present.

ABSORPTION SPECTRA OF WHOLE ROCK BEFORE AND AFTER HEATING AT 200-225°C FOR TWO HOURS

The effect of heating on the absorption spectrum of a polished interior section of Apollo 11 rock, 10017 has been published earlier (Hapke, et al (1970)). The heating at 200°C for two hours followed irradiation with ultraviolet light and X-rays. After standing, the effect is similar to heating pristine 10022 or 12018 pristine interior rock. Figure 1 shows the spectrum of rock 10022, 45 before heating and the change in the spectrum caused by heating at 200°C for two hours. The second spectrum is obtained by subtracting the spectrum taken before heating from one measured after heating. The result is a difference spectrum. Spectral bands below zero indicate a decrease in each given band appearing there. This is the result of a decrease in the specific absorbing ion causing the band. Thus one sees in Figure 1 a decrease in bands due to Fe^{3+}, Cr^{3+}, Ti^{3+} and Fe^{2+}. Rock 10022 (similarly 10017) contains little olivine but is rich in pyroxenes, plagioclase and ilmenite. The plagioclase is transparent in the region studied and the ilmenite is opaque. The absorption spectrum of this rock is due entirely to the pyroxene minerals present and changes upon heating are therefore changes in the pyroxene. The apparent decrease of the Fe^{2+} on heating is because of the interaction of neighboring Fe^{3+} and Fe^{2+}, probably across t2g orbitals. Thus decrease in the concentration of the Fe^{3+} causes an apparent decrease in the Fe^{2+} although the amount of Fe^{2+} is actually increasing slightly.

Figure 2 illustrates the difference spectrum of Apollo 12 rock 12018,50, an interior portion, upon heating at 200-225°C for two hours. The major effects noted are decreases in Fe^{3+} and Fe^{2+} bands. This rock contains both pyroxenes and olivine and thus the difference spectrum is more complex than in the other two rocks studied. Table 1 summarizes the bands found to decrease upon heating at 200-225°C in all three rocks. The transitions to which the bands are related will be discussed when the spectra of the individual minerals are presented. Two positive bands are observed in Figure 2 at 3.35 and 3.42 electron volts. A band due to Mn^{2+} appears in spodumene at 3.35 eV (unpublished work) and this may be a similar transition in lunar augite. The band at 3.42 may also be due to Mn^{2+}.

TABLE 1

NEGATIVE DIFFERENCE SPECTRA, AFTER HEATING AT 200-225°C
FOR 2 HOURS, ALL SPECIMENS APPROXIMATELY 30μ THICK

	Peak Maximum in Electron Volts		
ABSORBING ION	APOLLO 11 10017	APOLLO 11 10022	APOLLO 12 12018
Fe^{2+}	1.1	1.3	1.28, 1.37
Ti^{3+}	——	2.4	1.72, 2.46
Cr^{3+}	3.2, 3.53	3.5	1.82, 1.94, 3.20, 3.70, 4.06
Fe^{3+}	4.5	——	——
Cr^{3+}	4.8	4.8	5.28
Fe^{3+}	5.5	5.5	5.90
Ti^{4+}	tail > 6	tail > 6	tail > 6

2

The decrease of Fe^{3+}, Cr^{3+} and Ti^{3+} upon heating at relatively low temperature has been interpreted as reduction of the Fe^{3+} and Cr^{3+} accompanied by oxidation of the Ti^{3} according to the following equation:

$$Fe^{3+} + Cr^{3+} + 2Ti^{3+} \rightarrow Fe^{2+} + Cr^{2+} + 2Ti^{4+}$$

This reaction takes place in both pyroxenes and olivine as will be shown later.

An examination of the three rocks studied indicates that they have all cooled slowly. Under these conditions one expects to find the cations in the individual minerals in equilibrium. If this is true, one would not expect oxidation-reduction reactions to take place among the cations at a temperature as low as 200 to 225°C. It is known that natural α and β-radiation cause oxidation of Fe^{2+} in terrestrial minerals. β-radiation is more efficient than α-radiation. Cosmic rays are a rich source of secondary β-rays. Therefore it is suggested that both Fe^{2+} and Cr^{2+} are oxidized by secondary radiation from cosmic rays as well as by natural radioactivity present in the lunar rocks. A Ti^{4+} ion is reduced to Ti^{3+} for each Fe^{2+} and Cr^{2+} originally present in the rock that is oxidized to Fe^{3+} and Cr^{3+}. It is suggested that a major portion of these three ionic species are produced in the pyroxene and olivine of lunar rocks after the rocks have cooled and been subjected to subsequent radiation.

The conclusion that ferric iron was produced subsequent to the cooling of the rock is strengthened by the low oxygen fugacity found in lunar rocks and by the absence of magnetite.

The probable location of the ions, being oxidized or reduced, in the mineral structure will be suggested when the individual mineral is discussed.

SPECTRA OF PYROXENE IN ROCKS 12021 AND 12018

Rock 12021 has crystals of large size compared to Apollo 11 rocks. Some pyroxene grains have zones of differing color. These colored zones consist of a core of greenish yellow pigeonite rimmed with a brown zone of augite pyroxene. (Warner, J. 1970). The absorption spectrum of the pyroxene single-crystal measured in rock 12021,65 was a zoned crystal as described above. The spectrum is shown in figures 3 and 4 as a dashed curve. The absorption band maxima attributed to Fe^{2+} are listed in Table 2. The Fe^{2+} spectrum consists of two d-d transitions of Fe^{2+} in M_1 sites in the structure and two d-d transitions due to Fe^{2+} in M_2 sites. The configuration of the M_1 site is that of a regular octahedron and that of the M_2 site is that of a distorted polyhedron. Since one would expect the Fe^{2+} in an equivalent site in pigeonite to absorb energy at a lower value (longer wavelength) than in titanaugite, the M_1 and M_2 absorption bands are doubled (except for the M_1 transition at 1.41 eV) for transitions of Fe^{2+} in each of the two regions of the structurally-zoned pyroxene crystal. The charge-transfer band is also doubled, because of an energy-shift in the two zones of the crystal.

In the pyroxene structure one would ordinarily expect Fe^{3+} to favor M_1 positions and Fe^{2+} to favor M_2 positions. However, if the Fe^{3+} is caused by radiation damage it is not yet possible to predict whether a Fe^{2+} in an M_2 or M_1 site will be favored or whether the oxidation of Fe^{2+} to Fe^{3+} will be a random process favoring neither structural position.

Table 3 lists the Fe^{2+} bands in a wine-brown pyroxene in Apollo 12 rock 12018,50 after heating at 200-225°C for two hours. The pyroxene

TABLE 2

FERROUS ABSORPTION BANDS IN ZONED PYROXENE CRYSTAL FROM ROCK 12021,65

STRUCTURAL POSITION	BAND MAXIMUM IN ELECTRON VOLTS	ABSORBANCE	Δ CM^{-1}
M_2 - pigeonite	0.675	0.58	5440
M_2 - augite	0.75	0.49	6050
M_1 - pigeonite	1.19	0.66	9600
M_1 - augite	1.24	0.68	10,000
M_1 - pigeonite	1.29	0.85	10,405
M_2 - augite	1.34	0.81	10,810
M_1	1.41	0.76	11,370
charge transfer $Fe^{2+} \rightarrow Fe^{3+}$ Pigeonite	1.97	0.71	15,890
charge transfer $Fe^{2+} \rightarrow Fe^{3+}$ Augite	2.01	0.72	16,210

crystals in this rock are also relatively large. In the polished section studied, the best region of 2mm diameter was a clump of pyroxene crystals of the same color. The absorption spectrum of this clump of pyroxene crystals is shown in figures 3 and 4. These crystals are of the same thickness as the zoned-crystal in rock 12021. The intensity of the absorption is almost identical in the infra-red region as shown in figure 3. However, the Fe^{2+} spectrum is not doubled. In comparing the absorption peak positions to those listed in Table 2, one cannot choose whether the polycrystalline aggregate of crystals is pigeonite or augite.

The Fe^{3+} charge transfer band is so intense in the zoned pyroxene, it could not be measured. In the pyroxene in rock 12018 after heating, the intensity of the Fe^{3+} band has been reduced enough to be measured as shown in Table 3. It is not illustrated but is similar to the α-Fe^{3+} band in figure 1 before any heat treatment although of somewhat lower absorbance.

Tables 4 and 5 tabulate the absorption maxima of bands related to manganese that are too weak to be seen readily in the difference spectra of the whole rock; they are detectable in the spectra of the crystals of pyroxene and olivine. If the major portion of Fe^{3+} and Cr^{3+} are produced by oxidation of Fe^{2+} and Cr^{2+} respectively then the higher valence states which normally would favor M_1 positions may be in M_2 positions. The Fe^{3+} ($3d^5$) with zero crystal field stabilization energy would favor the M_1 site because of its smaller ionic size compared to Fe^{2+}. The Cr^{3+} ($3d^3$) ion would favor the M_1 sites both for crystal field and ionic size reasons. However Fe^{2+} ($3d^6$) and Cr^{2+} ($3d^4$) favor M_2 positions based on site distortion factors. Since the oxidized states are produced after the crystal has formed by radiation damage, one has Fe^{3+} in a Fe^{2+} site and Cr^{3+} in a Cr^{2+} site. These sites must undergo some local steric readjustment due to the change in cationic charge. The Ti^{4+} reduced to Ti^{3+} upon oxidation of the Fe^{2+} and Cr^{3+} may be in either silicon sites or M_1 sites or both, the M_1 site possibly being favored.

TABLE 3

FERROUS AND FERRIC ABSORPTION BANDS IN A POLY-CRYSTALLINE AGGREGATE OF PYROXENE FROM ROCK 12018,50 AFTER HEATING AT 200-225°C FOR TWO HOURS

ION	STRUCTURAL POSITION	BAND MAXIMUM IN ELECTRON VOLTS	ABSORBANCE	Δ CM^{-1}
Fe^{2+}	M_2	0.66	0.48	5,325
Fe^{2+}	M_1	1.265	0.78	10,205
Fe^{2+}	M_2	1.31	0.80	10,565
Fe^{2+}	M_1	1.38	0.80	11,130
Fe^{2+}	Charge Transfer $Fe^{2+} \rightarrow Fe^{3+}$	1.94	0.67	15,650
Fe^{3+}	Charge Transfer	5.635	2.54	45,450

TABLE 4

CHROMIC, TITANOUS, MANGANIC AND MANGANUS BANDS IN ZONED PYROXENE FROM ROCK 12021,65

ION	PROBABLE STRUCTURAL POSITION	TRANSITION	BAND MAXIMUM IN ELECTRON VOLTS	ABSORBANCE	Δ CM^{-1}
Cr^{3+}	M_1	d-d	1.85	0.65	14,920
Cr^{3+}	M_1	d-d	1.90	0.68	15,325
Cr^{3+}	M_1	Charge Transfer	3.95	2.02	31,860
Ti^{3+}	M_1	Charge Transfer	2.45	0.85	19,760
Mn^{3+}	M_1	d-d	2.28	0.76	18,390
Mn^{2+}	M_1	d-d	2.78	0.91	22,425
Mn^{2+}	M_1	d-d	2.89	0.92	23,310
Mn^{2+}	M_1	d-d	2.98	0.96	24,035

TABLE 5

CHROMIC, TITANOUS, MANGANIC AND MANGANOUS BANDS IN PYROXENE FROM ROCK 12018,50 AFTER HEATING AT 200-225°C FOR TWO HOURS

ION	PROBABLE STRUCTURAL POSITION	TRANSITION	BAND MAXIMUM IN ELECTRON VOLTS	ABSORBANCE	Δ CM^{-1}
Cr^{3+}	M_1	d-d	1.80	0.62	14,520
	M_1	d-d	1.89	0.64	15,245
	M_1	d-d	2.01	0.66	16,210
	M_1	Charge Transfer	2.95	0.82	23,795
	M_1	Charge Transfer	3.9	1.29	31,455
Ti^{3+}	M_1	Charge Transfer	1.75	0.615	14,115
	M_1	Charge Transfer	2.45	0.735	19,760
Mn^{3+}	M_1	d-d	2.28	0.68	18,390
Mn^{2+}	M_1	d-d	2.95	0.81	23,795

SPECTRA OF OLIVINES IN ROCKS 12021 AND 12018

The olivines in these two Apollo 12 rocks are the largest single crystals present. They are light yellow-green in color in 30 μ thickness. Figure 5 illustrates the Fe^{2+} spectrum of an olivine crystal in rock 12021,65 as found in the untreated rock and the spectrum of a single olivine crystal in rock 12018,50 after heating at 200-225°C for two hours. Tables 6 and 7 tabulate the Fe^{2+} band data for these two crystals. The transitions are all d-d except the charge transfer bands near 2.0 eV. There is a Fe^{3+} charge transfer band in the ultraviolet region in the olivine crystal in rock 12021,65 at 5.64 eV with an absorbance of 2.86. The Fe^{3+} band was too intense to measure in the heated olivine from rock 12018,50.

The M_1 structural position in olivine is that of a tetragonally distorted octahedron while the M_2 site has the configuration of a trigonally distorted octahedron. The Fe^{2+} ion tends to favor the M_2 position in olivine.

Tables 8 and 9 list the peaks of absorption bands attributed to Cr^{3+}, Ti^{3+}, Mn^{3+} and Mn^{2+} in the two olivines measured.

TABLE 6

FERROUS ABSORPTION BANDS IN OLIVINE IN ROCK 12021,65

STRUCTURAL POSITION	BAND MAXIMUM IN ELECTRON VOLTS	ABSORBANCE	Δ CM^{-1}
	0.66	0.68	5,325
M_2	1.18	0.52	9,520
M_1	1.34	1.08	10,810
M_1	1.62	0.51	13,065
Charge Transfer $Fe^{2+} \rightarrow Fe^{3+}$	2.00	0.54	16,130

TABLE 7

FERROUS ABSORPTION BANDS IN OLIVINE IN ROCK 12018,50 AFTER HEATING AT 200-225°C FOR TWO HOURS

STRUCTURAL POSITION	BAND MAXIMUM IN ELECTRON VOLTS	ABSORBANCE	Δ CM^{-1}
M_2	1.18	0.54	9,520
M_1	1.28	0.50	10,325
M_1	1.62	0.41	13,070
Charge Transfer $Fe^{2+} \rightarrow Fe^{3+}$	2.05	0.38	16,535

TABLE 8

CHROMIC, TITANOUS, MANGANIC AND MANGANOUS BANDS IN OLIVINE CRYSTAL IN ROCK 12021,65

ION	PROBABLE STRUCTURAL POSITION	TRANSITION	BAND MAXIMUM IN ELECTRON VOLTS	ABSORBANCE	Δ CM^{-1}
Cr^{3+}	M_1	d-d	1.77	0.51	14,275
Cr^{3+}	M_1	d-d	1.86	0.52	15,000
Cr^{3+}	M_1	Charge Transfer	4.00	1.67	32,265
Cr^{3+}		Charge Transfer	4.59	2.18	37,020
Ti^{3+}	M1	Charge Transfer $Ti^{3+} \rightarrow Ti^{4+}$	2.44	0.645	19,680
Mn^{3+}	M_1	d-d	2.30	0.58	18,550
Mn^{2+}	M_1	d-d	2.67	0.67	21,535

TABLE 9

CHROMIC, TITANOUS, MANGANIC AND MANGANOUS BANDS IN OLIVINE CRYSTAL IN ROCK 12018,50 AFTER HEATING AT 200-225°C FOR TWO HOURS

ION	PROBABLE STRUCTURAL POSITION	TRANSITION	BAND MAXIMUM IN ELECTRON VOLTS	ABSORBANCE	Δ CM^{-1}
Cr^{3+}	M_1	d-d	1.92	0.41	15,485
Cr^{3+}		Charge Transfer	3.24	0.55	26,135
Cr^{3+}		Charge Transfer	4.59	3.06	37,020
Ti^{3+}	M_1	Charge Transfer	1.71	0.41	13,790
Ti^{3+}	M_1	Charge Transfer $Ti^{3+} \rightarrow Ti^{4+}$	2.52	0.44	20,325
Mn^{3+}	M_1	d-d	2.38	0.40	19,195
Mn^{2+}	M_1	d-d	2.72	0.44	21,940
Mn^{2+}	M_1	d-d	3.06	0.50	24,680

TABLE 10

MINERAL SOURCE OF DIFFERENCE SPECTRAL BANDS IN ROCK 12018,50

ION	ROCK PEAKS IN eV (NEGATIVE)	PYROXENE PEAKS IN eV	OLIVINE PEAKS IN eV
Fe^{2+}	1.28	1.31	1.28
Fe^{2+}	1.37	1.38	1.41
Ti^{3+}	1.72	1.75	1.71
Cr^{3+}	1.82	1.80	—
Cr^{3+}	1.94	1.94	1.92
Ti^{3+}	2.46	2.45	2.52
Mn^{2+} (?)	2.99	2.95	3.06
Cr^{3+}	3.20	—	3.24
Cr^{3+}	3.70	—	—
Cr^{3+}	4.06	3.9	—
Cr^{3+}	5.28	—	4.59
Fe^{3+}	5.90	5.64	—
	(POSITIVE)		
Mn^{2+} (?)	3.35	—	—
Mn^{2+} (?)	3.42	—	—

Figure 6 illustrates the high intensity of the Cr^{3+} charge-transfer band at 4.00 eV (3100A) compared to the Ti^{3+} charge transfer band in olivine at 2.44 eV (5065A). The Cr^{3+} band not shown at 4.59 eV is still more intense. This figure indicates that Cr^{3+} is important in affecting the color on the ultraviolet side of the spectrum as well as Fe^{3+} in both olivine and pyroxene.

COMPARISON OF DIFFERENCE SPECTRUM OF ROCK 12018,50 TO SPECTRA OF PYROXENE AND OLIVINE

In Table 10, the negative peaks in the difference spectrum of rock 12018,50 after heating at 200-225°C for 2 hours is compared to the spectra of the individual pyroxene and olivine crystals in the same rock after heating. All peaks in the whole rock match peaks of either mineral or both minerals except the charge transfer peaks of Cr^{3+} (5.28) and Fe^{3+} (5.90) are shifted to higher energy. Also there is no Cr^{3+} peak at 3.7 in the minerals. The shift to higher energy in the deep ultraviolet may be apparent rather than real due to the increase of Ti^{4+} in the vacuum ultraviolet, the tail of which overlaps the Fe^{3+} and Cr^{3+} bands in the region 5-6eV, causing them to appear to be at higher energy. This is caused by the increase in Ti^{4+} band due to oxidation of the Ti^{3+} on heating. The entire reaction on heating at 200-225°C appears to be:

$$Fe^{3+} + Cr^{3+} + 3Ti^{3+} \ (+ Mn^{3+}) \rightarrow Fe^{2+} + Cr^{2+} + 3Ti^{4+} \ (+ Mn^{2+}).$$

The data on Mn^{2+} is uncertain and the positive bands in the difference spectrum of the whole rock at 3.35 and 3.42 eV have not been positively identified.

SPECTRUM OF PLAGIOCLASE IN ROCK 12021,65

The absorption spectrum of a single crystal of plagioclase in rock 12021,65 with dimensions 0.6mm x .2mm (x 30 microns thick) was measured. In the wavelength region 2000-17,500 A, there is no light

TABLE 11

ABSORPTION BANDS IN ORANGE GLASS FRAGMENT IN BRECCIATED ROCK 10048,44

ION	PROBABLE CONFIGURATION	TRANSITION	BAND MAXIMUM IN ELECTRON VOLTS	ABSORBANCE	Δ CM^{-1}
Fe^{2+}	octahedral	d-d	1.22	0.94	9,840
Fe^{2+}	octahedral	d-d	1.29	0.97	10,405
Fe^{2+}	octahedral	d-d	1.44	0.90	11,615
Fe^{2+}	octahedral	d-d	1.61	0.77	12,985
Fe^{2+}		Charge Transfer	1.98	0.97	15,970
Cr^{3+}	octahedral	d-d	1.80	0.84	14,520
Cr^{3+}	octahedral	d-d	1.86	0.87	15,000
Cr^{3+}	octahedral	d-d	1.93	0.94	15,565
Ti^{3+}	octahedral	Charge Transfer	1.69	0.78	13,630
Ti^{3+}	octahedral	Charge Transfer	2.48	1.52	20,005
Mn^{3+}	octahedral	d-d	2.33	1.44	18,795
Mn^{2+}	octahedral	d-d	2.18	1.33	10,725
Mn^{2+}	octahedral	d-d	2.75	1.63	22,180
Mn^{2+}	octahedral	d-d	2.85	1.67	22,985
Mn^{2+}	octahedral	d-d	2.91	1.71	23,390

absorption. The absence of the intense Fe^{3+} charge transfer band in the ultraviolet indicates that the Fe^{3+} ion in plagioclase is less than one ppm. The weakly absorbing Fe^{2+} could be present in the order of magnitude of 1000 ppm and not be detected. It is hoped to measure a thicker crystal of lunar plagioclase to see if any spectral bands can be observed.

THE ABSORPTION SPECTRUM OF A FRAGMENT OF ORANGE GLASS IN BRECCIATED ROCK 10048,44

This 150 micron diameter particle of orange glass in a polished section of breccia, 50 microns thick had the largest cross-section of any transparent material present. The glass fragment was roughly circular with a bright orange-red color in transmitted light. Figure 4 includes the spectrum of this glass in the visible region, the most prominent band is the $Fe^{2+} \rightarrow Fe^{3+}$ charge-transfer band with a maximum at 1.98 eV. Figure 7 shows the absorption spectrum of the glass in the infra-red region. A prominent vibrational band is present at 0.98 eV. The source of this band has not been identified. Table 11 lists the spectral bands present in this glass and the ions responsible. Due to the small size of the fragment, the spectrum could not be observed below 3.18 eV (3900A) because of its high intensity of absorption and the small amount of light transmitted by the small size of the fragment. Thus the ferric peak could not be observed although the 1.98 eV $Fe^{2+} \rightarrow Fe^{3+}$ charge-transfer band is present indicating that Fe^{3+} is present in the glass in sufficient quantity to interact with the Fe^{2+} ion.

CONCLUSIONS

Heating lunar basaltic rocks at low temperature in air causes reduction of Fe^{3+} and Cr^{3+} and oxidation of the Ti^{3+} in the pyroxenes and olivine present. It is probable that Mn^{3+} is present and reduced to Mn^{2+} by the mild heating at 200 to 225°C. It is suggested that Fe^{3+}, Cr^{3+}, and Mn^{3+} are reduced by such a mild heat treatment because they are not in equilibrium in the mineral structure. They are all in sites of the reduced species, viz a Fe^{2+} site is the location of Fe^{3+} in the structure. The structural site must readjust to a smaller cation with different bonding. Electroneutrality is preserved in the crystal by a Ti^{3+} being oxidized for each cation reduced by radiation. It is suggested that the most likely sources for the oxidation-reduction reactions are β-rays produced as secondaries following cosmic ray bombardment. Another source of β's is natural radioactivity present in the minerals. Since the rocks studied are from the interior of the rock, the effects of solar X-rays, ultraviolet light, and solar wind protons and electrons are negligible.

Absorption bands of Cr^{2+} were not detected in any of the specimens studied. Indications of Ti^{4+} were indicated by increase in the difference spectra of rocks in the deep ultraviolet upon oxidation of the Ti^{3+} present.

Deep-seated lunar rocks should be lower in Fe^{3+}, Cr^{3+}, and Ti^{3+} than surface rocks if the main source of the oxidation-reduction reactions is cosmic ray bombardment. The concentrations of these species should also increase with time of radiation by cosmic rays.

ACKNOWLEDGMENTS

This work was supported by grant NAS 9 9942 of the National Aeronautics and Space Administration. Mr. Grover Moreland of the National Museum of Natural History, Washington, D.C., is thanked for preparation of the polished sections of lunar rock used in this work. Mr. Ed Skopinski prepared the final drawings of the figures.

Professor S. Keith Runcorn is thanked for the invitation to present this paper at the Moon Symposium at the University of Newcastle upon Tyne.

REFERENCES

Hapke, B.W., Cohen, A.J., Cassidy, W.A., and Wells, E.N., (1970) Solar Radiation Effects on the Optical Properties of Apollo 11 samples, Proceedings of the Apollo 11 Lunar Science Conference Vol. 3, 2199-2212, Pergamon Press.

Warner, J. (1970), Apollo 12 Lunar-Sample Information NASA Technical Report R-353 p. 94-96.

Weeks, R.A., Kolopus, J.L., Kline D., and Chatelain, A., (1970) Nuclear Resonance of ^{27}Al and electron resonance of Fe and Mn, Proceedings of the Apollo 11 Lunar Science Conference Vol. 3, 2467-2490, Pergamon Press.